3. Lifetime Measurements

Larry J. Curtis

With 7 Figures

The beam-foil light source has a number of unique features which permit many new types of experiments. Some of these features are rather subtle, but the time-resolved nature of the decay process is so conspicuous that it is apparent why the first and most widely-applied usage of this technique should be in the measurement of atomic lifetimes. Because of the nearly monoenergetic properties of the beam, the time t since excitation directly corresponds to the distance from the foil x and is given by

$$t = x/v \quad , \tag{3.1}$$

where the beam velocity v is calculable from the beam energy E after the beam emerges from the foil and the atomic mass M of the ion from

$$v[\mathrm{mm/ns}] = 13.9\ (E/M)^{1/2}\ [\mathrm{MeV/amu}]^{1/2} \quad . \tag{3.2}$$

Thus the decrease in light intensity with distance from the foil for a spectrally resolved emission line is a measure of the rate of relaxation of the parent level, and directly leads to its mean life. In the absence of repopulation by cascading transitions from higher levels, this mean life is proportional to the negative inverse of the logarithmic derivative of the decay curve of the emitted light.

In addition to this obvious time-resolved nature, the beam-foil source possesses a number of other properties which are advantageous in lifetime determinations. Mass analysis of the ion beam assures that it is isotopically pure and free of contaminants. It has a very low particle density (typically 10^5 ions/cm^3) and thus exhibits no self-absorption, no collisional de-excitation and no inter-ionic field effects. Nearly any charge state of any element can be excited in this manner and studied using emitted optical, UV, or X-ray radiation, or, in some cases, electrons ejected through autoionization processes. The technique permits the study of multiply-excited states, which seem to be much more copiously populated in beam-foil excitation than in other sources. Coupled with these advantages are, of course, a number of disadvantages. The low particle density leads to low light levels (although the light per atom is probably very high compared to other sources). Doppler broadening of the in-flight

emitted radiation makes line blending a serious problem. The foil can undergo damage and change its properties slightly with time. The population is not selective, which complicates the decay-curve interpretation with cascade repopulation effects. Although some of these factors did introduce substantial uncertainties in some of the early beam-foil measurements, they have now been studied in great detail and methods have been developed to reduce or circumvent their effects. Thus recent beam-foil measurements must in general be considered as among the most extensive and most reliable lifetime determinations presently available.

As is evidenced by other chapters in this book, the beam-foil source often exhibits both coherent and anisotropic excitation. This has made possible many types of experiments involving fine and hyperfine structure and Stark and Zeeman effects. Improvements in spectral resolution have made possible term identifications and the measurement of Lamb shifts. The source can also be useful in the study of atomic collision and autoionization mechanisms. Thus beam-foil excitation is a very versatile technique, applicable to a broad range of studies. However, the in-flight decay of an excited ion is such a powerful technique for generating time-resolved decay curves, and foil collisions are so unique in their excitation properties, that lifetime determinations must remain one of the areas of primary emphasis in beam-foil spectroscopy.

In this chapter we shall describe the measurement of decay curves by the beam-foil technique (primarily in terms of optical photon emission), the extraction of mean lives from these decay curves, and the procedures which are utilized to assure reliability of the mean lives. The emphasis will always be on beam-foil measurements, but the techniques used for analysis are equally valid whether the decay curve is generated by in-flight decay of a beam excited by a foil, a gas stripper, or a laser beam, or by excitation of a gas cell by a pulsed or modulated electron beam, photon beam, or heavy-ion beam.

One word of caution is in order. A number of examples of possible pitfalls in beam-foil measurements are described in this chapter. The point of including these (often unlikely) troublesome cases is to indicate the degree to which beam-foil measurements can extract reliable mean lives even under difficult circumstances. The reader should recognize that modern beam-foil measurements routinely account for the points raised, and are free of such systematic errors.

3.1 Lifetime Studies as a Basic Area of Atomic Physics

Measurements of atomic lifetimes have become a very active research area in a field which was commonly treated as closed only a little over a decade ago. Although many

aspects of this development are more thoroughly treated elsewhere in this book, it is fitting that a discussion of lifetime measurements begin with a brief account of their importance and sudden emergence as a basic research area.

3.1.1 The Need for Lifetime Measurements

Lifetime measurements are needed both to improve fundamental knowledge of atomic structure and to meet specific needs in areas such as astrophysical abundance determinations, plasma diagnostics and optical excitation processes. Solar abundance determinations have been perhaps the most dramatic use of lifetime data, and estimates of solar abundances of iron-group and rare-earth-group elements have been changed by factors up to ten by beam-foil measurements. These measurements are particularly valuable because of the difficulties which the iron and rare-earth groups present to theoretical calculations. The current status of lifetime measurements and solar abundances is described in a recent review article by SMITH [3.1]. Lifetime measurements have also been useful in the determination of abundances in the interstellar medium from satellite data [3.2,3]. Sophisticated theoretical techniques have been developed for the calculation of atomic transition probabilities; these techniques require experimental determinations in order to select among various approximation techniques. These theoretical techniques have been reviewed by several authors [3.4-7], and are extensively treated in this volume also (see chapters 4 and 5). Lifetime data are particularly useful when they can be extrapolated along isoelectronic or homologous sequences [3.8,9], so that a well-placed measurement in one element can provide increased reliability for neighboring elements.

Most applications for atomic lifetime measurements are to specify emission and absorption of radiation under steady-state or dynamical circumstances, quite unlike the free-decay conditions under which a lifetime manifests itself so clearly. Therefore the lifetime results must (except for unbranched decays) be combined with branching-ratio data and presented in terms of spontaneous transition probabilities (A-values) and absorption oscillator strengths (f-values). These quantities are defined and their inter-relations presented in Subsection 3.2.2. It is possible to measure A-values and f-values directly by techniques such as emission from arcs and shock tubes, absorption by a vapor or slow atomic beam, and anomalous dispersion. However, these measurements require a knowledge of the density of the radiating atoms, which has been a source of considerable error, and are generally restricted to the neutral species and also to resonance transitions. A number of extensive review articles which compare the various methods for measuring lifetimes, A-values, and f-values are available [3.10-16]. Relative A-values and f-values can be measured more reliably than absolute values, and provide the necessary complement to lifetime measurements. Since a lifetime measurement compares only the intensity of a given transition with itself at different times, it requires a knowledge neither of the density of radiating particles

nor of the efficiency of the detection system. Thus lifetime measurements provide a highly reliable and indispensable overall normalization for A-value and f-value determinations.

3.1.2 Lifetime Measurements Prior to the Development of the Beam-Foil Technique

It is not possible to separate the development of atomic lifetime measurements from that of nuclear lifetime measurements, for it involves a succession of adaptations of nuclear discoveries and techniques to an atomic context.

Although the mathematical concepts of exponential growth and decay are as ancient as the geometric progression, and many examples of exponential and multiexponential processes exist in nature, measurement inaccuracies and the influence of external conditions prevented rate constants from being interpreted as fundamental properties of statistical processes until the discovery of radioactivity [3.17]. The nuclear exponential decay law was discovered by RUTHERFORD [3.18], when a gaseous decay product migrated from a natural radioactive source and decayed to lay a deposit on a nearby surface, thus producing a separated radioactive source with a lifetime of a few hours. In 1900 RUTHERFORD and SODDY [3.19-21] chemically separated a decay product with a lifetime of a few days from its long-lived parent and observed the recovery, or "growing in", within the parent. This established the importance of the cascade repopulated decay curve. RUTHERFORD and SODDY also introduced the concepts of a "half-life" and a "mean life" into the terminology in 1904 [3.22,23]. In 1905 VON SCHWEIDLER [3.24] showed that the exponential decay law can be deduced from the laws of chance with the assumptions that the probability of decay is constant in time and the same for all members of the same species. It is significant that it was in lifetime measurements that this first clear encounter with a process which is not accessible to causality occurred [3.25]. In 1910 BATEMAN [3.26] solved the set of coupled differential equations which describes the unbranched case of sequentially-cascaded decay, and these solutions were applied to the study of the natural radioactive series. It is interesting to note that the possibility of multiple direct cascading was ignored, since the natural radioactive chain members have at most one a-decay and one B-decay feeder level, which differ by many orders of magnitude in lifetimes. (This is to be contrasted with the application to atomic lifetimes, in which the earliest assumptions were that all cascading is direct. The subtleties of indirect cascading described in Subsection 3.6.1 have only recently been considered). Thus lifetimes were among the first nuclear properties to be systematically studied.

The use of lifetime measurements as an indicator of atomic structure has developed at a much slower pace than its nuclear counterpart. Atomic term-value analysis began with Kirchhoff and Bunsen in 1859, and by 1913 had been refined to the level of the Bohr atom. A few quantitative attempts to measure post-excitation radiation from

free atoms had been made by this time, such as the 1908 canal-ray studies of WIEN [3.27] and the 1913 work of DUNOYER [3.28], the latter of whom sent sodium atoms through a beam of sodium light and attempted unsuccessfully to photograph light from the emerging atoms. However, it was not until 1916 that the concept of an atomic disintegration constant was formally introduced by EINSTEIN [3.29,30], in an analysis of the atomic radiation process which was constructed in close analogy with nuclear radioactivity. A dynamical calculation of an atomic mean life was performed in 1919 by WIEN [3.31] which combined classical radiation theory with the Bohr atom. It is perhaps indicative of the general underestimation of the importance of atomic mean lives that the WIEN mean-life formula was forgotten, while the Bohr term-value formula appears in nearly all elementary atomic physics textbooks. WIEN's work has been reviewed and the terminology updated [3.32], and is worth recalling here. WIEN assumed that a quantum of energy becomes available after an electron passes from one allowed Bohr orbit to another, and is thus radiated from the latter orbit at constant centripetal acceleration. For circular orbits this yields

$$\tau = \frac{3\lambda^3\zeta^2}{16\pi^3\,\alpha c a_0^2 n_f^4} = \left(\frac{\lambda}{1004.33}\right)^3 \frac{\zeta^2}{n_f^4}\ [\mathrm{ns}] \quad , \tag{3.3}$$

where λ is the radiated wavelength measured in angstroms, ζ the net charge of the nucleus and core electrons, α the fine-structure constant, a_0 the Bohr radius, c the speed of light, and n_f the principal quantum number of the final orbit. This classical formula gives surprisingly accurate results [3.32] and can often provide a good first approximation. The quantum mechanical theory of transition probabilities was developed by DIRAC [3.33,34] in 1926, but mean-life measurements were not then considered a crucial test of quantum theory. However a number of measurements of mean lives were made, and it is noteworthy that in-flight decays of atomic beams were among the first methods used. WIEN [3.27,31,35] performed a series of experiments using in-flight decay of canal rays, which were the precursors of beam-foil and beam-gas spectroscopy. Similar canal-ray mean-life experiments were also performed by DEMPSTER [3.36,37] and others [3.38-42]. WALLERSTEIN [3.43] applied electric and magnetic fields to canal rays and observed the first excited beam quantum beats, but this technique fell dormant with the death of WIEN in 1928. In 1932 KOENIG and ELLETT [3.44] optically excited a thermal atomic beam and observed its in-flight decay in a geometry very much like that of a modern beam-laser experiment. Although this work was qualitatively repeated by SOLEILLET [3.45], this technique also fell into disuse. Early forms of pulsed-electron-beam gas excitation and Kerr-cell chopped-photon-beam excitation methods were also developed in the 1920's. A review of mean-life experiments performed prior to 1933 is given by MITCHELL and ZEMANSKY [3.10], and a perusal of these results attests to the lack of nanosecond time resolution so vital to atomic mean-life measurements. Thus the modern era of atomic mean-life measurements did not begin until after the development of nanosecond response phototubes and coincidence

circuits and their application to nuclear-physics measurements after World War II [3.46].

The first application of delayed-coincidence measurements to atomic mean lives was by HERON et al. [3.47,48], in a pulsed electron-beam experiment performed in 1954. However, they used a single-channel method which viewed only one fixed delay window at a time, and hence suffered from low detected intensity. A variation of this experiment was performed in 1955 by BRANNEN et al [3.49] who also used electron excitation, but with delayed coincidences between the cascade and primary photons. Again, single-channel techniques were used, and intensity problems were encountered. In 1961 BENNETT [3.50] adapted multichannel-analyzer techniques, developed in the mid-1950's for nuclear-physics applications, to pulsed electron-beam delayed-coincidence measurements. This provided an instrument which is equally sensitive to photons over a wide range of times after excitation, and greatly increased the usable intensity. In this form, this technique came into fairly wide use at the same time that beam-foil spectroscopy was being developed by KAY [3.51] and by BASHKIN [3.52], which ushered in the period of intense activity in mean-life measurement which is still in progress.

3.2 Definitions of Basic Quantities

Since the primary purpose of a mean-life measurement is to obtain atomic transition probabilities and absorption oscillator strengths, we shall list the relationships among these various quantities with particular emphasis upon their connection to a mean-life measurement. We use the nomenclature of CONDON and SHORTLEY [3.53], and denote an atomic level as corresponding to a given value of total angular momentum J, which in the absence of external fields consists of $(2J+1)$ degenerate states (or sublevels), each specified by a different projection M of the angular momentum along some prescribed axis (for our purposes, the beam direction). All other quantum numbers are denoted simply by y, and the set of levels which have the same γ is called a term. A transition between levels gives rise to a line, a transition between states is called a component, and a set of transitions between terms is a multiplet. For compactness, we shall generally denote a set of quantum numbers by a single subscript, and indicate in the text whether this refers to a state or to a level, or to both. An exception will occur in discussions of alignment and polarization in which the quantum numbers (γJM) will appear explicitly to avoid confusion.

3.2.1 Instantaneous Populations

It is standard practice in mean-life studies to speak of the instantaneous populations of the various decaying states and levels. This description is not always relevant for beam-foil excitation since the eigenstates which are populated by the source are

not necessarily the same as those of the radiative decay process. Thus the excitation Hamiltonian may not be diagonal in the representation which diagonalizes the decay Hamiltonian. The decaying states are then said to be coherently excited, and can exhibit quantum beats. Since we are primarily concerned here with measuring mean lives it is important to seek conditions which preclude quantum beats. We shall therefore restrict our discussions to situations in which (a) fine-structure levels are so distinct in energy that coherences between them are unlikely to take place, (b) the foil is axially symmetric about the beam so that there are no coherences between different M states [3.54], (c) there are no external fields to mix the states, and (d) hyperfine interactions are negligible. Under these circumstances there can be no coherences between states quantized with respect to the beam, and their individual state populations, as well as their combined level populations completely describe the excitation without recourse to density-matrix methods.

3.2.2 Transition Probabilities and Oscillator Strengths

In an emission process, the instantaneous rate of spontaneous photon emission $I_{u\ell}$ between an upper state or level u, to which N_u atoms are excited, and a lower state or level ℓ, is given by [3.29,30]

$$I_{u\ell} = N_u A_{u\ell} , \tag{3.4}$$

where $A_{u\ell}$ is the spontaneous transition probability. In an absorption process, N_ℓ atoms in a lower state or level ℓ are equivalent, in radiative absorption to the state or level u, to n classical harmonic oscillators given by [3.55]

$$n = N_\ell f_{\ell u} , \tag{3.5}$$

where $f_{\ell u}$ is the absorption oscillator strength. For transitions between levels, the quantities are related by

$$g_\ell f_{\ell u} = \frac{mc}{8\pi^2 e^2} A_{u\ell}^2 \; g_u A_u = \left(\frac{\lambda_{u\ell}}{2582.7}\right)^2 g_u A_{u\ell} , \tag{3.6}$$

where $A_{u\ell}$ is the transition wavelength in Angstrom units, g_u and g_ℓ are the degeneracies of the upper and lower levels, respectively, and $A_{u\ell}$ is measured in nanoseconds. For components, the expressions are the same, except the degeneracies do not appear. The mean life τ_u and its inverse α_u are defined according to

$$1/\tau_u \equiv \alpha_u \equiv \sum_\ell A_{u\ell} . \tag{3.7}$$

Thus f-values can be computed from inverse mean lives through the relationship

$$g_\ell f_{\ell u} = \left(\frac{\lambda_{u\ell}}{2582.7}\right)^2 g_u \left(\frac{A_{u\ell}}{\alpha_u}\right) \alpha_u \quad , \tag{3.8}$$

where $A_{u\ell}/\alpha_u$ is the relative branching ratio, which cannot be determined in a mean-life measurement and must be obtained through some other source. Inverse mean lives can be computed from f-values through the relationship

$$\alpha_u = \sum_\ell \left(\frac{582.7}{\lambda_{u\ell}}\right)^2 \frac{g_\ell f_{\ell u}}{g_u} \tag{3.9}$$

In theoretical calculations, it is convenient to define the line strength S, which is symmetric in emission and absorption. It is related to the transition probability by

$$S \propto (\lambda_{u\ell})^{2L+1} g_u A_{u\ell} \quad , \tag{3.10}$$

where L is the multipolarity of the emitted radiation. The proportionality constants for E1, M1, and E2 radiation are presented by SHORE and MENZEL [3.56,p.445]. Under the assumption of spin-orbit coupling, the line strength is the same for all levels in a multiplet [3.57], and if the A-value or f-value for one line in a multiplet is known, the values for all other lines in that multiplet can be obtained by appropriate wavelength and degeneracy corrections.

3.3 Measurement of Beam-Foil-Excited Decay Curves

Subsequent sections will describe refined techniques for extracting mean lives from decay curves. However, the most important part of any mean-life measurement lies not in the analysis, but in the experimental measurement itself, which must be designed to obtain the most reliable and informative decay-curve information possible.

3.3.1 Strengths and Limitations of the Beam-Foil Technique

Beam-foil excitation is by far the most widely used method of direct mean-life measurement, and more mean-life measurements have been made by this technique than by all other direct techniques combined. For example, a summary of transition probabilities for atomic absorption lines formed in interstellar clouds has recently been compiled by MORTON and SMITH [3.58], who cite 159 mean-life measurements of 101 multiplet transitions. Of these, 96 are beam-foil, 44 are modulated electron-beam phase-shift, 8 are pulsed electron-beam delayed-coincidence, 6 are modulated resonance-radiation phase-shift, 3 are high-field level-crossing and 2 are Hanle measurements. Further, the transitions in this compilation are not even particularly well suited to

beam-foil methods, since only 18 of the 101 transitions were in atoms more than once ionized. Similarly, LAUGHLIN and DALGARNO [3.59] have recently presented a comparison between theoretical calculations and experimental measurements of transition probabilities along isoelectronic sequences of Be, B and N, and cite 67 mean-life measurements of 24 transitions. Only 5 of these measurements were by methods other than beam-foil.

Thus, because of its wide use, beam-foil excitation is often applied to systems for which it is not the optimum technique available. For example, decay curves of transitions from singly-excited levels in neutral or singly-ionized atoms could in general be measured by pulsed-electron beam-gas delayed-coincidence techniques with much better wavelength resolution (hence less blending) and higher signal-to-noise ratios than are possible using beam-foil methods. One factor which militates against the beam-foil technique for the important case of neutral atoms is that very few neutrals emerge from a foil. Of course, the yield of neutrals is enhanced by working at the smallest possible particle velocity, but this introduces two serious handicaps. For one, beam scattering becomes especially serious. For another, foil life becomes quite short, particularly for heavy ions.

The alternative of the pulsed electron-beam method has been developed to a high degree of sophistication by a number of workers [3.60-63] which makes it an extremely attractive technique to complement beam-foil methods. This is particularly true in view of the developments introduced by ERMAN [3.16] in which high-frequency deflection techniques, combined with kilovolt electron beams, make possible nanosecond pulses at megahertz repetition rates with average currents of several milliamps during the pulse. The technique also has the advantage of a variable time window, so that long-lived components can be followed on one time scale, short-lived components on another, and a combined analysis performed. Thus, any transition which can be strongly excited by pulsed-electron beam-gas techniques can probably be more favorably measured by these techniques than by beam-foil methods, if appropriate equipment is available.

The mean lives which can be extracted from beam-foil decay curves are generally limited to the range from 10^{-6}s to 10^{-11}s, although values as short as 3.7×10^{-12}s have recently been reliably extracted by BARRETTE and DROUIN [3.64] using new high spatial resolution techniques. The beam velocity must lie between the speed of light and the slowest speed with which ions can emerge from the foil in a collimated beam. The measurable flight paths are between the shortest beam length resolvable by the optical system and the furthest downstream distance which can be viewed without beam spreading distortions or loss of the signal in the background. It must be kept in mind that a proper determination of a decay curve requires that one make measurements at a number of points. Thus a reasonable, practical limitation on the shortest beam length one can use is approximately 10 times the shortest resolvable length. These considerations have been examined by BROMANDER [3.65], who devised the plot shown below in

Fig.3.1 to illustrate the measurable mean-life ranges using various types of accelerators.

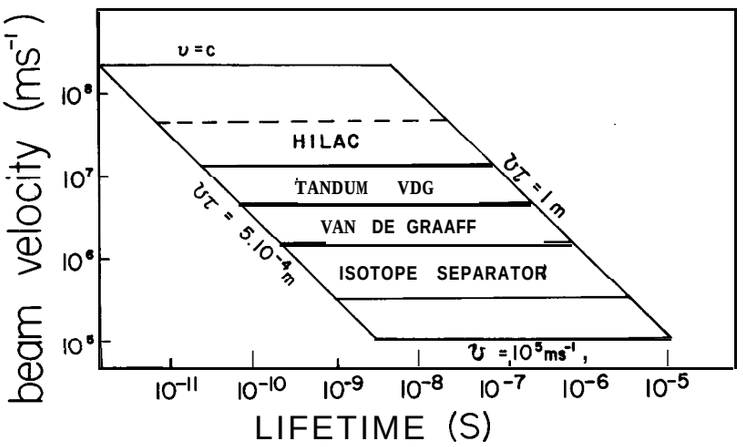

Fig.3.1 Limitations of the beam-foil technique for lifetime measurements. The ranges for the most commonly-used accelerators (Isotope separator, single-ended Van de Graaff, Tandem Van de Graaff and HILAC) are indicated. (Courtesy of Dr. J. Bromander [3.65])

Most of the weaknesses of the beam-foil technique are traceable either directly or indirectly to the low light levels involved, and could be eliminated if higher resolving power could be used. The strengths of the technique lie in the unparalleled ability of the beam-foil source to excite all types of ions to high ionization degrees, high excitation states, and multiply-excited states. For detailed descriptions of these areas, the reader is referred to recent review articles on beam-foil spectroscopy by MARTINSON and GAUPP [3.66], by BASHKIN [3.67], and by MARTINSON [3.68,69], and to a recent review article on multiply-excited states by BERRY [3.70].

3.3.2 Details of Beam-Foil Apparatus and Measurement Procedures

The widespread use of the beam-foil technique is probably due in part to the reasonably simple nature of the basic experimental apparatus, which is relatively inexpensive if a suitable accelerator facility is available. However, in the past several years rather sophisticated instrumentation and refined data-acquisition procedures have been incorporated into beam-foil lifetime measurements, which have substantially improved the accuracy of the data. Many of these techniques were developed primarily in efforts to resolve short-period quantum beats in fine- and hyperfine-structure measurements, and exceed normal requirements for mean-life work. Since quantum beats and

mean-life decay curves are often measured in the same laboratory on the same apparatus, this has led to a marked increase in the precision to which lifetime measurements are now routinely performed.

Modern beam-foil measurements are in sharp contrast to those of a decade ago, when the paucity of mean-life data justified order-of-magnitude estimates. Thus, in the early 1960's, a beam-foil study could provide valuable information by classifying level mean lives as "short", "medium", or "long" according to the length of a wavelength-dispersed photograph of the beam. As required accuracies have risen, measurement techniques have been refined, and the uncertainties in the earlier measurements must not be allowed to compromise the high reliability of modern beam-foil measurements.

Today, beam-foil decay-curves are usually obtained by stepwise translating the (5-20 $\mu g/cm^2$) foil [3.71] along the beam axis, referenced relative to a fixed point in the evacuated (10^{-6} tort-) foil chamber which is viewed by a high-speed optical system. The foil motion is achieved by a trolley which is driven by a precision machine screw with low backlash and high positional accuracy and reproducibility [3.72], often to within $\pm$ 0.05 mm. From 20 to 40 foils are mounted on a rotatable turret, and a given foil can be reproducibly selected by an external control dial and indicator. The foil-translation mechanism is usually driven by a stepping motor which is shaft encoded to provide a channel-advance signal to a multichannel analyzer operated in the multiscaling mode. The output of the optical detection system is thus accumulated in a separate scaling channel for each position of the foil relative to the viewed position. The step size (as short as 0.1 mm) and the total number of steps are programmable (in some laboratories they are controlled by an on-line computer), and the travel is recycled many times to signal-average any instrumental drifts, beam fluctuations, or foil aging. If the signal averaging is done over many cycles, the stepping motor can be advanced after equal amounts of time at each foil position. However, in order to remove the effects of beam fluctuations, the stepping-motor advance is more often gated by collection of a fixed amount of some monitoring quantity indicative of the instantaneous excitation to the level studied. One type of system uses the total beam charge collected in a Faraday cup, but this is sensitive to the average charge state leaving the foil; that average charge can change with foil aging. A more commonly-used system which avoids this problem collects light from the transition studied at a fixed distance from the foil, either directly by a foil-fixed phototube, or through a fiber optics link to a second monochromator and phototube. In either case, the signal either averages to the same total accumulation time in each channel, or a channel-by-channel dark-count correction is made.

The details of the optical system vary with the wavelength region, but single-photon detection techniques are used almost exclusively. For the optical wavelength region,

a lens focuses light onto the entrance slit of a monochromator from a segment of the beam often 0.1 mm or shorter in length. This resolution can be checked by quantum-beat measurements, and focus is often achieved by translating the foil past the optical system and minimizing the travel necessary for the light to rise from near extinction on the upstream side to its full value on the downstream side. When one views closer than 1 mm to the foil, the foil holder begins to vignette the collected light, so the sharpness of the rise does not indicate the actual spatial resolution. Since the light is not strong, a fast (low dispersion) monochromator is used, with low resolution to admit the Doppler-broadened spectral lines. The spectrometer is refocused to a moving source to minimize this broadening [3.73-76]. A low-noise photomultiplier tube is placed at the exit slit. Some photomultiplier tubes are cooled to reduce the dark-count rate to a few per second. In the vacuum UV wavelength region, a lens can not be used, but grating masks are used to limit the beam length viewed, and channel electron multipliers or sodium-salicylate-coated photomultiplier tubes serve as photon detectors. The optical system usually views at an angle 90" with the beam, but occasionally an oblique angle is used to follow a very short mean life into the foil.

The system described above is typical of most modern beam-foil laboratories and, although the specific details may vary somewhat, it should provide a general guide to the procedures presently used. A representative modern beam-foil decay-curve is shown in Fig.3.2.

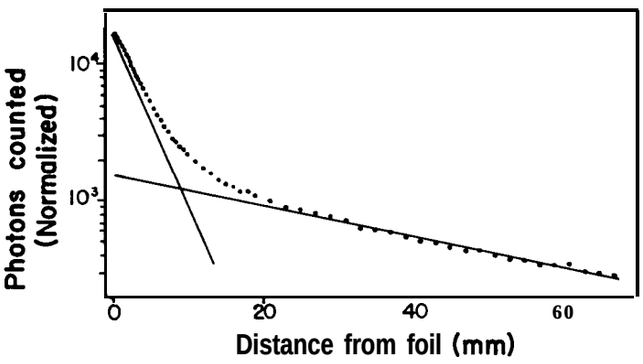

Fig.3.2 Representative beam-foil intensity decay-curve for the 2348Å Be I line ($2s^2\ ^1S - 2s2p\ ^1P$) measured at 180 keV ion energy [3.144]

A number of possible pitfalls exist which are carefully examined as part of any measurement. One such problem involves the fact that the foil characteristics change slightly during bombardment. It was observed by CHUPP et al. [3.77] that the energy

thickness of the foil increases with bombardment. This was investigated by BICKEL and BUCHTA [3.78], who determined that for an 80 keV Li^+ ion beam incident upon a carbon foil, the foil increased its thickness at 2.7 $\mu g/cm^2$/hour. At energies for which the energy loss in the foil is a reasonable fraction of the total beam energy, foils are therefore replaced often and energy analyses are made frequently. The foil also broadens the beam velocity distribution. Errors introduced into mean lives by beam velocity straggling and beam spreading due to interaction with the foil have been investigated by CURTIS et al. [3.79] and by KAY [3.80], who present calculations which indicate that these effects are negligible, even at rather low beam velocities. The possibility that beam spreading could cause ions to escape from the viewing volume has been studied by ETHERTON et al. [3.81]. They found that by placing a chamber-fixed beam collimator just upstream of the spectrometer slit and monitoring on Faraday cup current, these effects became negligible even at distances corresponding to more than 70 ns from the foil. The most important foil-dependent quantity requiring accurate determination is the average velocity of the foil-emergent particles. Several methods for its determination are available. A post-foil electrostatic energy analyzer [3.82] is one common method. Another method utilizes the Doppler shift of the in-flight emitted spectral line when viewed at a skew angle to the beam [3.83]. It is also possible to determine the velocity by a measurement of a precisely known quantum-beat frequency. Some beam-foil laboratories have facilities for beam pulsing [3.84] which permit the use of delayed-coincidence time-of-flight measurements to determine foil-emergent particle velocities. Another common approach is to calibrate the accelerator energy, using various nuclear resonances and thresholds [3.85]. The thickness of the foil can then be determined by optical transmission [3.86] or proton energy-loss measurements and the energy loss of the ion in the foil computed from theoretical estimates [3.87-89]. However, there is some indication that the theoretical estimates are not directly applicable to the beam-foil case, and may overestimate losses due to ions scattered in nuclear encounters, which tend to be removed from the forward-going beam [3.90]. This is particularly crucial in the case of very heavy ions, where the energy loss in the foil may be an appreciable fraction of the total energy, and researchers usually choose one of the direct velocity measurement techniques for such work.

Another problem involves line blending. Since the beam-foil source requires fast optics and wide acceptance angles viewing a moving source, severe Doppler broadening is unavoidable. Thus there is a chance, particularly for rich spectra, that the tails of neighboring lines will overlap with the line measured, adding unrelated components to the decay curve of interest. A number of approaches to this problem are available. The spectrum can be examined for blending under conditions which can reduce Doppler widths [3.66,Table 3] even though these conditions are not themselves suitable to lifetime determinations. If the decay is branched, or is part of a multiplet, the

various branches or related lines can be separately measured and compared. The decay curve can also be measured for equivalent times both on and off the line peak; slow-varying backgrounds should vanish from the difference between these measurements [3.91]. Thus the effects of line blending may occasionally lead to increased uncertainties in lifetimes, but that is probably not the most serious limitation brought about by blending. It is unfortunate that the possibilities of blending generally restrict the application of the beam-foil source to strong lines, which stand up above the tails of neighboring lines, and to lines which are well separated from their neighbors.

One of the most widely discussed problems in beam-foil excitation involves cascade repopulation of the levels, which introduces the mean lives of higher-lying levels into the time dependence of the decay of each level. The analysis of these effects has been greatly aided by improved measurement techniques. Sub-millimeter spatial resolution and closely-spaced data points, together with low-noise detection equipment which permits measurement far out onto the decay-curve tails, have made possible very elegant numerical analyses. The general problem of cascade effects is described in detail in the next subsection, where we shall see that an adequate allowance for cascading in beam-foil measurements can be made in all but the most unusual circumstances. These rare cases where cascade effects can be serious and methods for handling them are discussed in Section 3.6.

Thus the quality of beam-foil decay-curve measurements has undergone a vast improvement in recent years, both in terms of the sensitivity of its instrumentation and in the procedures which are routinely performed to assure reliability. The low light intensities do not permit signal-to-noise ratios as favorable as in sources such as electron beam excitation, but with sufficient data accumulation time, decay curves of comparable quality can be obtained.

3.3.3 Cascade Repopulation - A Tractable Problem

As we saw in subsection 3.1.2, the problem of cascade repopulation has been familiar since the discovery of radioactivity, but for practical reasons the measurement of lifetimes in atomic systems greatly enlarges cascade contributions. This can be seen by observing that atomic mean lives usually lie between the nanosecond and the millisecond range, while the mean lives of the natural radioactive series range from half a microsecond to 20 billion years. Thus mean lives of cascade-coupled atomic levels are much more likely to overlap on a given time scale. Further, atomic systems have more closely spaced levels with fewer transitions forbidden by selection rules than are generally found in nuclei. Thus, multiple direct cascading, while common in atomic systems, is virtually non-existent in natural radioactivity.

The atomic cascade problem was discussed by WIEN [3.35,p.435] in 1927 and is present in essentially all generally applicable atomic excitation sources, and efforts to

eliminate it often introduce problems much more serious than cascading. For example, the pulsed-electron beam-gas source can be made cascade-free by the use of threshold excitation, which excites no levels above the level of interest. This has a number of drawbacks. In particular, excitation cross sections become vanishingly small near threshold, and light outputs are not sufficient unless high gas pressures are used, which introduce the possibilities of collisional de-excitation and radiation trapping. BENNETT and KINDLMANN [3.92] have made such measurements for neon, and DONNELLY et al. [3.93] have used this technique with noble-gas ions, but it has not been generally applied to other elements. Another technique to eliminate cascade effects from electron beam-gas excitation studies is to measure delayed coincidences between the cascade photon and the photon from the level of interest [3.94,95]. Again the cascades are eliminated at great cost, with the true coincidence rates down by 3 to 4 orders of magnitude from the singles rates. Still a third technique measures delayed coincidences between the inelastically-scattered electron beam and the decay photon [3.96]. This technique, although promising, requires an experimental system of considerable complexity, and has had limited application, primarily in neutral gases and molecules.

In modulated electron-beam phase-shift measurements, the cascades are studied through the frequency dependence of the phase shift. Analysis often treats the system as if only a single direct cascade were present, which is not a probable situation. The general relationship for the phase shift as a function of frequency for an arbitrarily cascaded and blended level has been calculated by CURTIS and SMITH [3.97], but computer simulations indicate that present experimental accuracies are not sufficient to extract more than one or two cascades from phase-frequency curves.

Excitation by optical radiation can eliminate cascades, but this generally provides access only to levels optically connected to the ground state or to metastable states. When resonance fluorescence techniques such as the Hanle effect and high-field level-crossing are extended to study non-resonance transitions through electron-beam or beam-foil methods, they also acquire cascade repopulation effects. DUFAY [3.98] has formally computed the cascade contributions to the Hanle effect. However, to evaluate the extent to which cascades affect these techniques requires a knowledge of the alignment and transfer of alignment of the cascade levels. It is sometimes conjectured that the transfer of alignment in these cases is slight, but the situation is extremely difficult to analyze quantitatively.

Despite the fact that cascades are a comparable problem in nearly every type of mean-life measurement, the words "cascade errors" have become synonymous with the beam-foil source. This is unfortunate in view of the high accuracy of modern beam-foil measurements, and is partially due to the extreme care with which beam-foil experimenters have approached the cascade problem. Other measuring techniques are often beset with

so many problems (pressure dependence, sample purity, rf pickup, etc.), that the cascades become of secondary importance. In beam-foil work, these problems are absent, and only the cascades remain, so they are carefully discussed in each paper.

There are a few cases of beam-foil measurements made prior to 1971 which lacked a sufficient dynamic time range and missed subnanosecond components or very long-lived cascades. Some values were thus reported which substantially overestimated the true mean lives. Most of these values have now been revised by subsequent remeasurements, so some care must be taken as to the origin of a given mean life to be sure that it is the currently accepted result. However, there are certain small trends which are important to consider.

In a report of their recent calculations, LAUGHLIN and DALGARNO [3.59] present a comparison of experimental and theoretical mean lives for a number of isoelectronic sequences, and report that, "The experimentally-determined transition probabilities are invariably smaller than our theoretical values." They attribute this to possible beam-foil cascade effects, so it is valuable to investigate the size, statistical significance, and possible origins of any such trend. PINNINGTON et al. [3.99] have examined the ratios of experimental to theoretical mean-life values for beam-foil measurements made in the University of Alberta Laboratory during the past four years. Their results are presented in Table 3.1, along with a similar set of ratios obtained

Table 3.1 Ratio of beam-foil mean-life measurement to theoretical mean-life computation for two unselected samples. The uncertainties are the sample standard deviations; sample size is given in parentheses

Source	$\tau_{BFS}/\tau_{Theor.}$
PINNINGTON et al. [3.99]	
(a) All values	1.24 ± 0.88 (47)
(b) Highest ratio excluded	1.11 ± 0.18 (46)
LAUGHLIN and DALGARNO [3.59]	
(a) All values	1.23 ± 0.51 (24)
(b) Highest ratio excluded	1.12 ± 0.16 (23)

from the compilation of LAUGHLIN and DALGARNO. Although all ratios are in fact greater than one, their values are within one standard deviation of that value. Further, most of the individual ratios were within 10% of unity, with only a few cases (2 of 71) in major disagreement. Therefore we must distinguish between two types of possible experimental errors: gross errors due to ambiguities in identifying mean lives (see

Subsection 3.6.1), which are difficult to typify in quoted uncertainties, and small errors, which are correctly typified by quoted uncertainties (usually 10%). In the vast majority of beam-foil decay curves today the cascade mean lives can either be resolved by a properly designed experiment, or else are too weak to affect the decay curve significantly. While the total neglect of cascading would certainly overestimate primary mean lives, there is no reason to believe that an exponential decomposition of a decay curve is more likely to undercorrect for cascading than to overcorrect for it. Thus, although cascading increases uncertainties, other sources of systematic error must be considered if the results in Table 3.1 constitute a meaningful discrepancy. For example, beam-foil measurements do contain a selection bias, since they can usually be performed only for strong transitions. Thus any theoretical approximation techniques which are especially applicable to strong transitions should be closely examined, as should trends in lifetimes measured by techniques equally applicable to strong and weak transitions. Also, DALGARNO [3.100] has pointed out that theoretical first-order 1/Z extrapolations along isoelectronic sequences uniformly underestimate mean lives, and gradient corrections have caused upward revisions for the higher members of the sequences [3.101]. WEINHOLD [3.102] and ANDERSON and WEINHOLD [3.103] have suggested a technique for calculating upper and lower bounds to theoretical transition probabilities, which, although generally very broad, could provide a useful guide. Such estimates, together with critical evaluations of the exciting mean-life measurements, could resolve the question of whether the small trends in Table 3.1 have significance. However, it must be stressed that we can probably be 95% confident that a mean-life measurement obtained from the beam-foil method in its modern form is reliable to within its statistical error or 10%, whichever is greater [3.99].

3.4 Time Dependence of the Measured Decay Curves

The mean-life determinations discussed in this chapter involve a measurement of the time-dependence of the radiation emitted by a relaxing atomic level. The mean life of the level is directly determined from this decay curve through analytical expressions which will be developed in this section. These expressions are applicable not only to beam-foil measurements, but also to decay curves generated under a wide variety of excitation conditions.

3.4.1 Solution of the Driven Coupled Linear Rate Equations

Most techniques for the direct measurement of atomic mean lives involve a study of the time-dependence of the radiation emitted by a sample during or subsequent to an external current density, Q(t), which generates the excitation. Usually, low densities are used so that collisional effects and radiation trapping within the sample

are negligible. In such cases, the instantaneous population $N_n(t)$ of a state or level n is governed by the equation

$$dN_n/dt = \sigma_n Q(t) + \sum_j N_j(t)A_{jn} - N_n(t)\alpha_n \quad , \tag{3.11}$$

where σ_n is the excitation cross section, A_{jn} is the transition probability for a cascade from the states or levels j, and α_n is the inverse mean life of the level n. This equation has an integrating factor, $\exp(\alpha_n t)$, which permits conversion to the form

$$\frac{d}{dt}\left[N_n(t)\exp(\alpha_n t)\right] = \exp(\alpha_n t)\left[\sigma_n Q(t) + \sum_j N_j(t)A_{jn}\right] \quad . \tag{3.12}$$

This differential equation can be changed to a convenient integral equation by integrating both sides between the limits minus infinity (when it is assumed that none of the excited states n is populated) and an arbitrary time t, shifting the integration variable and exchanging orders of integration and summation to obtain

$$N_n(t) = \sigma_n L_n(t) + \sum_j A_{jn}\int_0^\infty dt' \exp(-\alpha_n t')N_j(t-t'), \tag{3.13}$$

where the quantity $L_i(t)$ is the Laplace Transform Convolution of the excitation stimulus

$$L_i(t) \equiv \int_0^\infty dt' \exp(-\alpha_i t')Q(t-t'), \tag{3.14}$$

which has the very useful reduction property [3.104,105]

$$\int_0^\infty dt' \exp(-\alpha_j t')L_i(t-t') = [L_i(t)-L_j(t)]/(\alpha_j-\alpha_i) \tag{3.15}$$

For $i=j$, l'Hôpital's rule yields $-\partial L_i/\partial\alpha_i$ for the right-hand side of (3.15).

A relationship of the form of (3.13) holds for each state or level of the system, and the simultaneous solution of the coupled differential equations of a given state with those of its cascades can be performed to specify the instantaneous populations completely. The solution can conveniently be written in a closed-form series decomposition [3.104,105], in which the individual terms can be identified with cascades which contribute to the primary state or level through a specific number of intermediate states or levels. This series can be very neatly generated through an iterative process. As a zeroth approximation we neglect all cascades in (3.13) and obtain $N_n^{(o)}(t) = \sigma_n L_n(t)$. We then use this result to make the first approximation, which neglects cascades into cascades, and sets $N_j^{(o)}(t) = \sigma_j L_j(t)$ in (3.13). The integrals of $L_j(t)$ are easily reduced through the properties of (3.15), and we are ready to substitute this first approximation into (3.13) to obtain a second approximation. This process

is repeated until cascading up to a desired order is included, thus generating an expression, which, containing linear terms in the $L_i(t)$ quantities as its only time-dependence, can be written in the form

$$N_n(t) = \sigma_n L_n(t) + \sum_j \{j \to n\} + \sum_{kj} \{k \to j \to n\} + \sum_{\ell kj} |\ell \to k \to j \to n\}$$
$$+ \ldots + \sum \ldots \sum \{m \to (r \text{ steps}) \to n\} \quad , \tag{3.16a}$$

where the quantities in braces are diagrammatic symbols for the various functions which are generic to cascades of a given order. One can show that [3.104,105]

$$\{j \to n\} \equiv \sigma_j A_{jn} \left[\frac{L_n(t)}{(\alpha_j - \alpha_n)} + \frac{L_j(t)}{(\alpha_n - \alpha_j)} \right]$$

$$\{k \to j \to n\} \equiv \sigma_k A_{kj} A_{jn} \left[\frac{L_n(t)}{(\alpha_j - \alpha_n)(\alpha_k - \alpha_n)} + \frac{L_j(t)}{(\alpha_k - \alpha_j)(\alpha_n - \alpha_j)} + \frac{L_k(t)}{(\alpha_n - \alpha_k)(\alpha_j - \alpha_k)} \right]$$

$$\{\ell \to k \to j \to n\} \equiv \sigma_\ell A_{\ell k} A_{kj} A_{jn} \left[\frac{L_n(t)}{(\alpha_j - \alpha_n)(\alpha_k - \alpha_n)(\alpha_\ell - \alpha_n)} + \frac{L_j(t)}{(\alpha_k - \alpha_j)(\alpha_\ell - \alpha_j)(\alpha_n - \alpha_j)} \right.$$
$$\left. + \frac{L_k(t)}{(\alpha_\ell - \alpha_k)(\alpha_n - \alpha_k)(\alpha_j - \alpha_k)} + \frac{L_\ell(t)}{(\alpha_n - \alpha_\ell)(\alpha_j - \alpha_\ell)(\alpha_k - \alpha_\ell)} \right] \quad , \tag{3.16b}$$

which can be generalized to the form

$$\{m \to .. (r \text{ steps}) .. \to n\} \equiv \sigma_m A_{mb} \ldots A_{jn} \sum_{i=n}^{m} \left[L_i(t) / \prod_{j \neq i} (\alpha_j - \alpha_i) \right] \quad .$$

Here i and j range over the (r+1) cascade and primary states or levels and the product of transition probabilities is over the r-step cascade chain. Equation (3.16a) can be refactored into the form

$$N_n(t) = \sum_j \beta_{nj} L_j(t) \quad , \tag{3.17}$$

where the sum includes one term for the primary level n, and one term for every level which cascades, either directly or indirectly, into it.

In the following discussion, the variables are redefined in dimensionless form. For the beam-foil source, the excitation may be considered an impulse $Q(t) \propto \delta(t)$, so if we make the following replacements in (3.16)

$$L_i(t) \to \exp(-\alpha_i t)$$

$$\sigma_i \to N_i(0) \quad , \tag{3.18}$$

we obtain a specific expression for the population of any arbitrarily-cascaded beam-foil-excited level.

Three-level examples in which there are two repopulating cascades are often used for illustrative purposes, so we shall present them explicitly here. For a primary level labeled 1, repopulated by cascades from levels labeled 2 and 3, (3.16) and (3.17) yield a relationship

$$N_1(t) = [N_1(0)-\beta_{12}-\beta_{13}]\exp(-\alpha_1 t) + \beta_{12}\exp(-\alpha_2 t) + \beta_{13}\exp(-\alpha_3 t) \quad . \tag{3.19}$$

There are two possible schemes by which this can occur:

Case 1 Direct cascades - both 2 and 3 have transitions to 1, but are not themselves repopulated

$$\beta_{12} = N_2(0)\, A_{21}/(\alpha_1-\alpha_2) \quad ,$$

$$\beta_{13} = N_3(0)\, A_{31}/(\alpha_1-\alpha_3) \quad . \tag{3.20}$$

Case 2 Indirect cascades - 3 cascades into 2, which cascades into 1

$$\beta_{12} = [N_2(0) + N_3(0)A_{32}/(\alpha_3-\alpha_2)]A_{21}/(\alpha_1-\alpha_2)$$

$$\beta_{13} = N_3(0)A_{32}A_{21}/[(\alpha_1-\alpha_3)(\alpha_2-\alpha_3)] \quad . \tag{3.21}$$

As noted in Subsection 3.1.2, the indirect cascading case (with $N_1(0) = N_2(0) = 0$) was first deduced by RUTHERFORD and SODDY in their study of radioactive decay and recovery curves. The implications of direct and indirect cascading will be contrasted in Subsection 3.6.1.

The condition of (3.18) also describes the decay curves for all excitation sources which have a finite shut-off time after which $Q(t)=0$ (for example, a pulsed beam-gas source) provided $t=0$ is interpreted to be after shut-off. Equation (3.16) can also be applied to extract mean lives from driven excitation, with the only difference being that $L_i(t)$ becomes a more complicated function. For example, for a unit Gaussian driving stimulus $Q(t) = (h/\sqrt{\pi})\exp(-h^2t^2)$, the function becomes [3.104-106]

$$L_i(t) = \exp(-\alpha_i t+\alpha_i^2/4h^2)\,[1+\mathrm{erf}(ht-\alpha_i/2h)]/2 \quad . \tag{3.22}$$

Similarly, the empirical shape of a measured excitation pulse Q(t) (the "prompt" curve) can be numerically convoluted to form $L_i(t)$, which can then be inserted into

(3.16). This generalizes to arbitrary cascading a technique used by LAWRENCE [3.107] to extract short mean lives in pulsed-electron beam-gas excitation, and by HELMAN [3.108] in the analysis of fast luminescence behavior. For a unit step function, $L_i(t)$ is given by [3.104,105]

$$L_i(t) = [1 - \exp(-\alpha_i t)]/\alpha_i \quad . \tag{3.23}$$

Insertion of this relationship into (3.16) generalizes to arbitrary cascading the solutions developed by ANKUDINOV et al. [3.109,110] to describe excitation of a beam by a gas cell. This type of analysis is also extended in [3.104,105] to specify the phase shift for a modulated beam-gas excitation source, with arbitrarily complicated cascading included. Thus by evaluation of the single representative integral of (3.14), a surprisingly simple description of nearly any atomic relaxation process is given by (3.16).

3.4.2 A Quantitative Indicator of Level Repopulation - The Replenishment Ratio

Since cascade repopulation is a source of much concern in nearly all mean-life measurements, it would be useful if a reported mean-life determination could be accompanied by some estimate of the degree to which cascading was present. A convenient indicator is provided by the replenishment ratio [3.79], which is defined as the ratio of the cascade repopulation rate to the decay depopulation rate. From (3.11) this can be seen to be

$$R(t) \equiv \left(\sum_j N_j(t) A_{jn}\right) \Big/ \left(N_n(t)\alpha_n\right) \quad . \tag{3.24}$$

It is a positive quantity: $R(t)<<1$ implies there is little cascading; $R(t)>1$ indicates a growing-in behavior. For an undriven case, $Q(t)=0$, and (3.11) can be written

$$-d(\ell n\, N_n)/dt = \alpha_n[1-R(t)] \quad , \tag{3.25}$$

clearly exposing the fact that α_n is the upper limit to the negative logarithmic derivative of the decay curve (see subsection 3.6.1). In terms of the exponential sum of (3.17) the initial value of the replenishment ratio is given by

$$R(0) = \sum_j (1-\alpha_j/\alpha_n)\, \beta_{nj} \Big/ \sum_k \beta_{nk} \quad , \tag{3.26}$$

which is a convenient form for computation from curve fits.

3.4.3 Intensity Relationships for an Aligned Source

The intensity of radiation which is emitted into all 4π steradians in a given spontaneous transition is proportional to the instantaneous population of the upper state

or level, as shown in (3.4). However, in practice, a detector samples the radiation in only some limited solid angle, and has a sensitivity to the radiation's polarization. Thus, if the states are not equally populated, the differing angular patterns of the polarized component radiation can cause the time-dependence of the sampled line radiation and that of its corresponding level population to differ.

In the discussion of the relationship between component radiation and line radiation, most authors (e.g., [3.53,p.97] and [3.56,p.443] assume "natural excitation", or equal populations among the sublevels. This is a poor assumption for beam foil work, but fortunately not a necessary one since all sublevels must have the same mean life. Thus the line intensity emitted into all 4π steradians

$$I_{\gamma J,\gamma' J'} = \sum_{M}\sum_{M'} N_{\gamma JM} A_{\gamma JM,\gamma' J' M'} \tag{3.27}$$

can be written as a product of the level population,

$$N_{\gamma J} = \sum_{M} N_{\gamma JM} \quad , \tag{3.28}$$

and the line transition probability,

$$A_{\gamma J,\gamma' J'} = \sum_{M'} A_{\gamma JM,\gamma' J' M'} \quad , \tag{3.29}$$

since the sum of component transition probabilities taken over lower states is independent of the upper state. Thus (3.4) is valid for both lines and components if all radiation is included.

To describe a realistic experimental situation, let us consider the electric dipole radiated intensities AI' and $\Delta I^{\perp}$ detected at an angle θ to the beam through linear polarizers set parallel and perpendicular to the beam-photon plane. These intensities can be written in terms of the Zeeman components $\Delta M=0$ and $\Delta M=\pm 1$ as

$$AI'' = \eta_{\lambda}^{\parallel} \sum_{M} N_{\gamma JM}[A_{\gamma JM,\gamma' J' M} (2-3\cos^2\theta) + A_{\gamma J,\gamma' J'}(\cos^2\theta)] \tag{3.30a}$$

$$\Delta I^{\perp} = \eta_{\lambda}^{\perp} \sum_{M} N_{\gamma JM}[A_{\gamma J,\gamma' J'} - A_{\gamma JM,\gamma' J' M}] \quad , \tag{3.30b}$$

where $\eta_{\lambda}^{\parallel}$ and $\eta_{\lambda}^{\perp}$ are the detection efficiencies at the wavelength λ. Sum rules were used to write the $\Delta M=\pm 1$ components in terms of the line and $\Delta M=0$ A-values. The $\Delta M=0$ A-value has the useful property

$$\sum_{M} A_{\gamma JM,\gamma' J' M} = (2J+1)\, A_{\gamma J,\gamma' J'}/3 \quad , \tag{3.31}$$

from which one can easily recover AI' = $\Delta I^{\perp}$ for the natural excitation case, in which $N_{\gamma JM} = N_{\gamma J}/(2J+1)$. Thus the total radiation detected in a standard beam-foil arrangement at $\theta=90°$ is given by the sum of (3.30a) and (3.30b)

$$\Delta I = \sum_{M} N_{\gamma JM}[(2\eta_{\lambda}^{\parallel} - \eta_{\lambda}^{\perp})A_{\gamma JM,\gamma'J'M} + \eta_{\lambda}^{\perp} A_{\gamma J,\gamma'J'}] \quad . \tag{3.32}$$

Thus, unless $\eta_{\lambda}^{\perp} = 2\eta_{\lambda}^{\parallel}$, the intensity is not proportional to the total level population, but rather to a weighted sum of the sublevel populations.

Since all states of a level have the same mean life, the same mean lives will be contained in all component decay curves of a line. However, due to differences in sublevel populations, the admixtures of exponentials in the various components may differ, and the admixture of (3.32) will in general not correspond to that of the total radiation of any component, or to that of the line. This fact has implications which we shall discuss in the next subsection and in succeeding sections.

3.4.4 Distortions Which Preserve the Mean-Life Content of a Decay Curve

In Subsection 3.3.2 methods were described which can eliminate instrumental effects which could distort the decay curves from their multiexponential form. There are other classes of distortions inherent in all decay-curve measurements which do not affect the mean-life content of the curve, but do alter the admixture of exponentials. These distortions are important to consider, for although some analysis techniques (see Section 3.5) are sensitive only to the individual exponential components, others (see Section 3.6) rely on the detailed shape of the decay curve. It is possible to estimate the magnitude of these distortions and correct for them, as well as to adjust experimental conditions so as to eliminate them.

a) *Finite Time Window* The measured data are instrumentally integrated over some finite resolution time t. For a beam-foil source, this corresponds to the beam segment viewed by the optical system divided by the beam velocity; for a delayed coincidence measurement, it is the channel width (for a beam-foil source, At can be less than the channel width AT, which is the step size). The average value of the population over this interval is

$$\overline{N_n(t)} = \int_{t-\Delta t/2}^{t+\Delta t/2} dt'\ N_n(t')/\Delta t \quad . \tag{3.33}$$

Using (3.17) and (3.18) this becomes [3.111]

$$\overline{N_n(t)} = \sum_{j} \beta_{nj}[\sinh(\tfrac{1}{2}\alpha_j\Delta t)/(\tfrac{1}{2}\alpha_j\Delta t)] \exp(-\alpha_j t) \quad . \tag{3.34}$$

The admixture of exponentials is altered if the resolution width approaches any of the contributing mean lives.

b) *Finite Solid Angle* If the source is aligned, the intensity ΔI which enters a solid angle at 90° to the beam direction is given by (3.32). If we insert (3.17) and (3.18) we obtain

$$\Delta I = \sum_j \left\{ \sum_M \beta_{(\gamma JM)j} \left[(2\eta_\lambda^{\parallel} - \eta_\lambda^{\perp}) A_{\gamma JM,\gamma'J'M} + \eta_\lambda^{\perp} A_{\gamma J,\gamma'J'} \right] \right\} \exp(-\alpha_j t) \quad , \qquad (3.35)$$

so, unless every β is independent of M, we again have an exponential admixture which is different from that describing the level population [3.112]. Since the coefficient in braces involves the transition probabilities, the admixture can differ among the various branches of the decay, due to differing angular distributions of the same total intensity. This dependence can be eliminated by forcing $\eta_\lambda^{\perp} \to 2\eta_\lambda^{\parallel}$. This can be achieved by measuring each decay curve both in parallel and in perpendicular polarized light, correcting for the instrumental polarizations, and forming $\Delta I^{\parallel}/\eta_\lambda^{\parallel} + 2\Delta I^{\perp}/\eta_\lambda^{\perp}$. The same result can be attained by viewing the source through a linear polarizer with its axis inclined at the "magic angle" $\cos^{-1}(1/\sqrt{3}) = 54.7°$ to the beam-photon plane [3.113]. The polarizer will then pass 1/3 of the parallel and 2/3 of the perpendicularly-polarized light, which gives the desired result for a detection system which has no instrumental polarization. Instrumental polarization can be reduced to less than 1% by use of a polarization scrambler, which creates pseudo-depolarized light after polarization analysis [3.114].

With both polarizations viewed at an angle θ to the beam direction by a detection system with no instrumental polarization, we obtain, adding (3.30a) to (3.30b), with $\eta_\lambda^{\parallel} = \eta_\lambda^{\perp}$, and the substitution of (3.17) and (3.18),

$$\Delta I = \sum_j \left\{ \sum_M \beta_{(\gamma JM)j} \left[A_{\gamma JM,\gamma'J'M}(1-3\cos^2\theta) + A_{\gamma J,\gamma'J'}(1+\cos^2\theta) \right] \right\} \exp(-\alpha_j t) \quad . \qquad (3.36)$$

Thus even without instrumental polarization, the geometrical detection efficiencies cause the admixture to differ from that of N,(t) in a manner dependent upon alignment, branch, and angle. An exception occurs if the radiation is viewed at the "magic angle" to the beam, defined as above to be $\theta_M = 54.7°$, for which the component transition probability drops out and the M sum over β becomes unweighted.

It should be emphasized that the distortions discussed above change only the admixture of the exponentials, and not the exponential mean lives themselves. Thus an analysis which simply fits exponentials will not be affected by these distortions, but they must be considered in more sophisticated techniques which utilize cascade relationships between jointly-analyzed decay curves.

3.5 Mean-Life Extraction by Exponential Fits to Individual Decay Curves

The customary method for determining mean lives consists of approximating the decay curve of the desired level through the adjustment of the C_j and α_j parameters in the fitting function $\bar{I}$

$$\bar{I} \equiv \sum_j C_j \exp(-\alpha_j t) \quad . \tag{3.37}$$

As we have seen, an atomic decay curve is usually a multiexponential sum with a very large number of terms. However, in practice it is often sufficient to include only one or two cascade exponentials to obtain a good approximation of the primary mean life. The cascade mean lives obtained in such a fit should be considered averaged effective values, which do not necessarily correspond to any specific level. However, experiences with detailed cascade analyses (see section 3.6) have shown that there are cases in which one or two cascades completely dominate the repopulation, and are reliably recoverable from the decay-curve fit.

Nearly any analysis of exponential mean lives begins with a graphical plot on semilog paper, with the mean-life components resolved by repeated subtraction of straight lines. This curve-peeling approach can in some cases yield reliable results, but its limitations in accuracy due to cumulative error buildup should be apparent. However, the graphical method is still commonly used to obtain reasonable starting values for the computer programs which will be described here.

3.5.1 Maximum Likelihood Method

The maximum likelihood method utilizes the likelihood function L [3.115] defined as

$$L \equiv \prod_{i=1}^{N} \left[\bar{I}(C_1, C_2, \ldots \alpha_1, \alpha_2, \ldots t_i) / \int_{(t)} dt\, \bar{I} \right] \quad , \tag{3.38}$$

where $\bar{I}$ is defined in (3.37), the product is over i individual counts, each registered at a time t_i, and the integration extends over the entire measurable time window. The fit is accomplished by varying the parameters in such a way as to maximize L. Since the equations are non-linear, this requires a brute-force search. Computer programs have been developed which achieve maximization by the MALIK [3.116] stepping procedure, as well as by an alternative iteration procedure [3.117]. Provisions have been made to accept grouped multichannel data by correcting for the fact that the decay shifts the count centroid away from the channel centroid [3.118-120]. A modification has also been suggested [3.121] in which (3.37) is rewritten in terms of an alternative parametrization $C_j \rightarrow C'_j \alpha_j$. The correlation between C'_j and α_j is weaker than between C_j and α_j, which speeds the convergence. Use of these maximum-likelihood programs has been limited to one or two exponentials with constant background terms.

3.5.2 Non-Linear Least Squares Method

The most frequently-used technique is the method of least squares, which involves a minimization of the quantity [3.122]

$$S^2 = \sum_i [I(t_i) - \bar{I}\,(C_1, C_2, \ldots \alpha_1, \alpha_2, \ldots t_i)]^2\, w_i \quad . \tag{3.39}$$

Here $I(t_i)$ is the number of counts in channel i, t_i is the time centroid of channel i, $\bar{I}$ is the fitting function of (3.37), W_i is the uncertainty weight in the measurement of $I(t_i)$, and i is summed over channels. Minimization of S^2 is equivalent to maximization of L if the measured values are gaussian distributed about the parent distribution. For Poisson statistics, the best fit is not obtained by minimizing this mean square deviation from the mean since the Poisson distribution is always skewed below the mean, particularly so for counts less than around 100. Thus it is sometimes desirable to pool several channels on the decay curve tails in making this analysis.

Again, since (3.37) is not linear in the α_j parameters, neither L nor S^2 can be optimized by analytical differentiation and inversion (unless only a single exponential contributes, in which case the logarithmic intensities can be linearly fitted). Thus minimization must be achieved through numerical search methods, such as the method of steepest descent or the Gauss-Seidel linearization (Taylor Series). Since each of these techniques has a characteristic efficiency which depends upon the proximity to minimization, they are often combined through a scheme such as Marquardt's Algorithm [3.123] (the maximum-neighborhood method). If a true minimum is achieved, the resulting fitting parameters are independent of how the minimum was located and various programs should differ only in the time and number of iterations required for convergence. Weighted non-linear least-squares fitting programs are contained in the systems libraries of most large computer installations (e.g., [3.124-126]), and most packages already include an exponential sum as an optional function. Special programs of this type have also been developed specifically for use in mean-life data reduction (e.g., [3.127,128]). The amount of programming required is substantial, and most laboratories adapt an existing library program.

Although the fits should be independent of the specific search program, they are often quite sensitive to the weights chosen. For convenience, the weights are based on the measured data rather than the parent distribution and include a number of different sources of uncertainty. Since a decay curve begins with a high number of counts and often ends when the signal becomes comparable with fluctuations in the background, the local accuracies over the decay curve are expected to vary greatly. Statistical fluctuations are often not sufficient to account for the observed spread of data points, particularly in the high count region, where statistical inaccuracies may be only 0.1%, and non-statistical errors must be considered. A possible weighting which includes an incoherent sum of statistical and non-statistical errors is given by

$$W_i = I\{t_i) + [\varepsilon I(t_i)]^2 + 2B_i\}^{-1} \qquad (3.40)$$

Here ε is a small number, chosen so that $(W_i)^{-1/2}$ will match the spread of data points for large $I(t_i)$ while contributing a negligible amount for small $I(t_i)$, and B_i denotes any measured backgrounds which have been pre-subtracted to give $I(t_i)$. (The background may arise from several separate Poisson-distributed contributions, since such a merger is also Poisson-distributed with a mean equal to the sum of the separate means). If the fit is found to be sensitive to ε, a detailed study of non-statistical errors is necessary. In a modern beam-foil measurement, such as was described in subsection 3.3, non-statistical errors have largely been removed and statistical weights are usually sufficient. If weights are correctly chosen and properly normalized, the sample variance can be compared with that of a parent gaussian distribution of the same number of degrees of freedom (the number of data points minus the number of fitting parameters) by the χ^2 test [3.122]. The number of exponential terms which must be included for an adequate but not overparameterized fit can be selected by comparing the values of S^2 for various inclusions with a table of corresponding χ^2 probabilities [3.122]. The uncertainties in the individual parameters (for either the least-squares or maximum-likelihood methods) can be estimated by examining χ^2 as a function of each parameter in the neighborhood of the minimum.

It is seldom that beam-foil decay curves can be fitted to more than three exponentials (six free parameters). One limitation is imposed by the finite time-window (as shown in Fig.3.1; it is difficult to resolve times shorter than 0.05 ns or longer than 100 ns within a standard beam-foil chamber). Thus, only under unlikely circumstances could four exponential mean lives all differ from each other by at least an order of magnitude, and thus have a region of dominance within the measured decay curve. In pulsed beam-gas excitation, it is possible to vary the duty cycle and examine the decay curve in various time domains [3.16], but even here it is difficult to extract the same four exponentials from two separate but equivalent measurements of a decay curve. LANCZOS [3.129] has studied the numerical implications of the exceedingly non-orthogonal properties of the exponential functions, and has noted extraordinary sensitivity of the fitted parameters to small changes in the data. This causes difficulties in applications to physical problems, where the aim of the fits is not merely to approximate the data closely by a mathematical function, but to determine accurately the physically meaningful parameters. LANCZOS estimates that to fit four or five exponentials would require measurement accuracies of from 6 to 8 significant figures, which is quite unrealistic when compared to actual measurement accuracies. However, in normal mean-life determinations, the situation is not as hopeless as this analysis would imply, since we desire accuracy in only one fitted parameter, the primary level's mean life. If this mean life dominates the decay curve, the fact that nonphysical values are recovered for the other parameters is not serious. The LANCZOS

caveat must certainly be heeded in attempts to extract cascade mean lives or relative initial populations from decay-curve fits.

The knowledge that the decay curve is a sum of exponentials, which have special analytical properties, is not incorporated into the basic fitting process. It is possible to utilize these properties, either in conjunction with a traditional fit, or in alternative fitting procedures, and partially counteract the disadvantages of non-orthogonality.

3.5.3 Differentiation and Integration of Decay Curves

One aspect of the exponential function which is not contained in the basic fitting procedure but which can sometimes increase the reliability of a fit involves its very simple properties under differentiation and integration. The derivative of (3.37) is

$$d\bar{I}/dt = -\sum_i (C_i\alpha_i) \exp(-\alpha_i t) \qquad (3.41)$$

while its integral from to to infinity is

$$\int_t^\infty dt'\bar{I}(t') = \sum_j (C_j/\alpha_j) \exp(-\alpha_j t) \quad . \qquad (3.42)$$

Therefore the differentiated and integrated decay curves should contain the same mean lives, but with coefficients which differ in a predictable way. This can be coupled with the fact that the early and the late portions of a decay curve are usually quite different in information content. The early portions contain short-lived exponentials and have high statistical accuracy, while the late portions contain long-lived exponentials and have low statistical accuracy. If the early portion possesses sufficient statistical accuracy to permit numerical differentiation [3.130], the process will further enhance the short-lived components and eliminate entirely the necessity for a constant background subtraction. Similarly, if the late portion can be integrated (this requires an accurate background subtraction and an extrapolation of the integration beyond the end of the decay curve, which can be done iteratively [3.50,p.28]) the long-lived exponentials will be further enhanced, and the integration will reduce the statistical fluctuations. The fitting procedure can be performed three times: once for the raw decay curve, once for the early portion of the differentiated curve, and once for the late portion of the integrated decay curve. An example [3.131] is shown in Fig.3.3. Agreement among the coefficients and mean lives in the various fits indicates the exponential content has been correctly described, and disagreement can indicate that an inappropriate number of exponential terms was used.

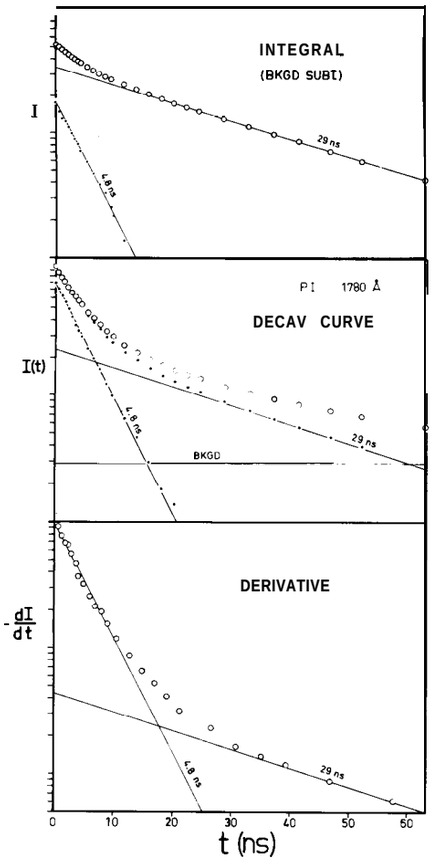

Fig.3.3 Curve fits to a measured decay curve (central figure) and its numerical integral (top figure) and derivative (bottom figure) for the 4s ^4P level in P I. All fits contain the same exponential lifetimes, but the admixtures vary in proportion to the relative lifetimes

3.5.4 Expansion About a Close-Lying Mean Life

In some cases, beam-foil decay curves appear to be relatively free of cascades. The question then arises of whether they really are cascade-free, or merely an effective sum of close-lying values. As we shall show in Subsection 3.6.1, there are situations in which this question is virtually impossible to answer. However, there are fitting techniques which are especially sensitive to small lifetime differences which can be used in such cases. As was pointed out by DENIS et al. [3.132], if (3.16) is Taylor-expanded about $\alpha_j = \alpha_n + \Delta\alpha$ for a contribution from a single direct cascade j, the equation becomes

$$N_n(t) = \exp(-\alpha_n t)\,[N_n(0) + N_j(0)A_{jn}(t-\Delta\alpha t^2/2) + \ldots] \qquad (3.43)$$

and a polynomial linear fit to the quantity $I_{nf}(t)\exp(\alpha_n t)$ (using the value α_n from a single exponential fit) can very sensitively expose small differences in mean life. ERMAN [3.16] has studied the problem in the context of pulsed-electron beam-gas excitation and has concluded that (barring the unlikely situations described in Subsection 3.6.1) it can introduce at worst a few percent error. If the cascade lifetime differed from the primary by more than this amount, the decay data would exhibit measurable curvature. If the lifetimes differed by less, the fitted value would be between the primary and cascade mean lives.

3.5.5 Fourier-Transform Methods

An alternative procedure has been developed by GARDNER et al. [3.133] in which the exponential sum over a discret set of mean lives is re-expressed as a Laplace integral over a continuous set of mean lives

$$I(t) = \sum_j C_j \exp(-\alpha_j t) \rightarrow \int_0^\infty d\alpha\, g(\alpha)\, \exp(-\alpha t) \quad , \qquad (3.44a)$$

where

$$g(\alpha) \equiv \sum_j C_j \delta(\alpha-\alpha_j) \quad , \qquad (3.44b)$$

and the function g(a) takes the form of a frequency spectrum with peaks of height C_j centered on the values α_j. Here $g(\alpha)$ can be computed through the inversion of this integral equation, and since $g(\alpha)$ has entirely different properties from I(t), this approach may avoid some of the problems created by the non-orthogonality of the exponential sum. Since inverse Laplace transform calculations for empirical functions present practical problems [3.108], a method of inversion using Fourier transforms was employed [3.133], which has been extended to permit the use of modern Fast Fourier Transform Algorithms [3.134] by SCHLESINGER [3.135]. Unfortunately this method requires the observation of all decays for many mean lives, and is seriously limited when more restricted ranges must be used. Another disadvantage is that the uncertainties in the parameters are difficult to estimate. The technique has not generally been applied to atomic mean-life work, but at the least it could provide useful starting values for an exponential search program.

3.5.6 Method of Moments

Another technique which transforms exponential data into an alternative form has been developed by BAY [3.136,137] and extended to include several exponentials by DYSON and ISENBERG [3.138], ISENBERG and DYSON [3.139], and SCHUYLER and ISENBERG [3.140]. Moments of the decay curve are numerically computed over the range of measured data

$$u_k \equiv \int_0^T dt\ t^k I(t) \quad , \tag{3.45}$$

where k runs from 0 to one less than twice the number of exponentials in the fitting function (so as to match the number of parameters). The fitting function (3.37) is also integrated and becomes (corrected for truncation)

$$\overline{u_k}\ (C_1, C_2, \ldots \alpha_1, \alpha_2, \ldots k) = \sum_j C_j \left[k!/\alpha_j^{k+1} - \int_T^\infty dt\ t^k \exp(-\alpha_j t) \right] \quad , \tag{3.46}$$

and a least-squares fit is made to the moments

$$S^2 = \sum_k [u_k - \overline{u_k}\ (C_1, C_2, \ldots \alpha_1, \alpha_2, \ldots k)]^2 \tag{3.47}$$

The infinite integrals in the fitting function can be generated recursively, but this correction usually contributes only a small perturbation in the fit. In order to integrate the data reliably, a special numerical filter was developed [3.138-140] to remove the high-frequency noise components. The technique has been successfully used to analyze simulated three-component decay curves, and an extensive review of the method and its application to biological systems is given by YGUERABIDE [3.141].

3.6 Mean-Life Extraction by Joint Analysis of Cascade-Related Decay Curves

In the previous section, analysis techniques were discussed by which mean lives are extracted from individual decay curves. These methods are in general highly reliable and provide a conclusive determination in most cases. However, there are a few situations in which the extraction is either particularly difficult, or for which there is an ambiguity in the assignment of the fitted mean lives. In such cases, it is possible to utilize additional conditions between cascade-related decay curves to sharpen the determination and to remove the ambiguities. We shall therefore discuss a few of the most difficult possible situations, and describe the techniques by which even these examples become tractable.

3.6.1 Ambiguities in the Assignment of Fitted Mean Lives

It is known [3.142] that substitution of certain combinations of decay rates and initial populations into (3.16) will remove the exponential term corresponding to the primary mean life. For example, if $N_3(0):N_2(0):N_1(0) = 5:3:1$ and $\alpha_3:\alpha_2:\alpha_1 = 3:8:27$ (unbranched) then (3.21) yields $\beta_{12} = 0$ and $\beta_{13} = N_1(0)$ and a single exponential results, although three different mean lives are involved. We mention this to show that a single exponential does not necessarily preclude cascades nor unambiguously determine mean lives.

The primary mean life can be extracted even if it is not among the fitted exponentials. This mean life may not be exhibited explicitly as an exponential, but it is nonetheless manifested implicitly through the relative coefficients of the cascade and primary admixtures, if both decay curves are measured. The decay curve $N_1(t)$, containing only the exponentials present in its direct cascade, and presenting a less drastic example which clearly illustrates the above point, is shown in Fig.3.4.

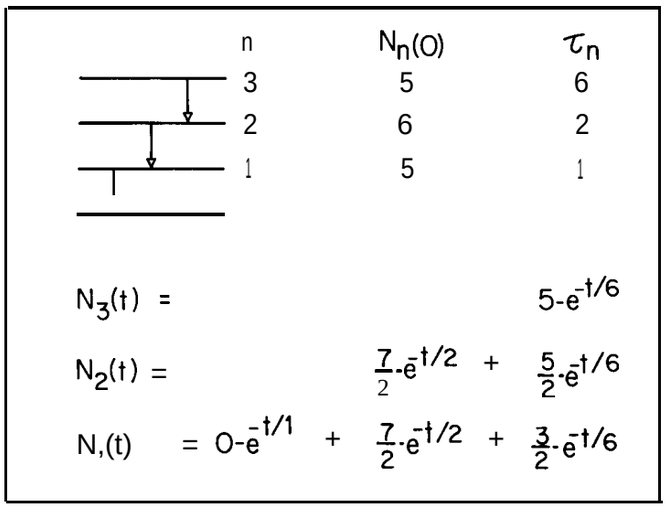

Fig.3.4 Example of an indirectly-cascaded level with a decay curve which does not involve the lifetime of that level. Although that lifetime does not appear as an exponential in any of the decay curves, it can be extracted from a comparison of the admixtures

In such a two-level example, the differential equation,

$$dN_1/dt = N_2(t)A_{21} - N_1(t)\alpha_1 \quad , \tag{3.48}$$

couples the solutions of (3.17) and (3.18) to yield the relationship

$$\frac{\beta_{22}}{\beta_{23}} = \frac{\alpha_1-\alpha_2}{\alpha_1-\alpha_3}\,\frac{\beta_{12}}{\beta_{13}} \quad , \tag{3.49}$$

and α_1 can be evaluated from the ratios of the coefficients and the cascade mean lives. Such implicit information can be utilized to analyze a wider class of situations in which the primary exponential term, although not fortuitously zero, is small, due either to heavy cascading or to a short mean life. Generalized techniques to extract

mean lives from cascade-coupled sets of decay curves will be described in the following subsections.

A frequently-cited example in which ambiguities in the assignment of mean lives occur is the "growing-in" decay curve. In this situation, one or more of the exponential coefficients is negative, and a maximum may occur in the decay curve or in one of its derivatives. If we examine the possibilities for such an occurrence in the absence of indirect cascades, (3.19) and (3.20) admit two possibilities: a short-lived primary level of low initial population, or a cascade level which is shorter-lived than the primary. Selection between these possibilities is called the direct cascade "growing-in ambiguity". Unfortunately, such ambiguities are not restricted to growing-in decay curves.

If a level were repopulated only by direct cascades, it would follow from the above that the primary mean life would be equal to or shorter than the shortest fitted mean life which has a positive coefficient. Thus in the absence of growings-in, the primary would always be the fastest contributor. Although this has been found generally to be the case, it is not a rigorously valid condition if indirect cascading is present. An example is given in Fig.3.5 of an indirect cascade scheme in which the primary level is of intermediate mean life, but exhibits no growing-in.

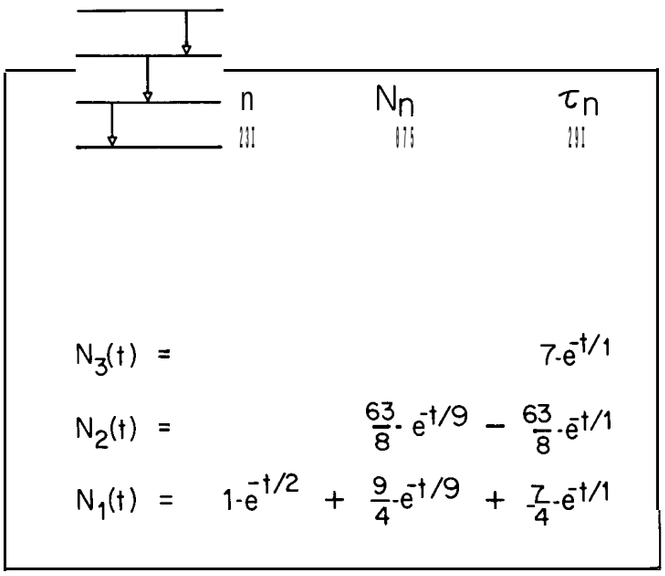

Fig.3.5 An example of a decay curve in which a cascade is the fastest contributing lifetime, but no negative "growing-in" coefficients are exhibited

Again, the ambiguity can be resolved if the cascade decay curves are also measured. Despite this counter-example to the "fastest non-growing-in" argument, it is still possible to establish a rigorous upper limit to the level mean life by examination of the logarithmic derivative of the decay curve. Since the replenishment ratio cannot be negative, (3.25) implies that

$$-d(\ell n\, N_n)/dt \leq \alpha_n \quad . \tag{3.50}$$

KAY [3.143] has shown that this inequality is valid, regardless of cascading conditions, instrumental time-resolution, detection efficiency, data-pointspacing,or velocity-dispersion effects. Although the situations described above may seem formidable, they are handled rather easily, if the decay curves of the cascade levels are also accessible to measurement, by techniques which are described in the subsections to follow.

3.6.2 Constrained Fits

One technique for incorporating measured cascade information into the analysis is the constrained fit. The decay curves of contributing cascades are measured and fitted by non-linear least-squares methods. Decay constants from the strongest lines observed in the cascades are then forced into the fitting function of the primary decay-curve least-squares fit, but the cascade mean-life values are fixed and only their coefficients are allowed to vary freely in the fit. Since these coefficients are linear parameters in the fit, they do not display the non-orthogonal behavior of the mean-life fits, and their use can account for a higher complexity of cascading than would otherwise be possible. MARTINSON et al. [3.144] have used this technique to fix up to five cascade mean lives in Be I decay curves. TIELERT and BUKOW [3.145] have developed a technique which minimizes the joint χ^2 for two measured decay curves which contain common mean lives, and have thus analyzed hydrogen decay curves including the effects of five mean lives, only one of which was free to vary. Although their analysis was primarily intended to determine the coefficients for population determinations, it recovered a highly reliable value for the free mean life.

3.6.3 Linearly-Fitted Normalizations of Cascade-Related Decay Curves

The constrained-fit methods described above use only the information that cascade exponentials are also contained in the primary decay curve, and ignore the relationships among the coefficients of the various admixtures which are imposed by the population equations, such as (3.49). This does have certain advantages, since mean lives are independent of excitation conditions and coefficients are not, so decay curves measured under quite different circumstances can be combined by a constrained fit. However, if we impose the additional condition that the primary level and all of its significant cascade levels are observed under equivalent excitation conditions, then their populations are coupled by the differential equation

$$dN_n/dt = \sum_j N_j(t)A_{jn} - N,(t) \text{ an} \quad . \tag{3.51}$$

If the decay curves are measured under circumstances such that they are free of all types of distortions including those discussed in Subsection 3.4.4, and are corrected to remove all background and blend contributions, then the decay intensity $I_k(t)$ (observed in any decay branch) is proportional to the instantaneous population of the decaying level k

$$I_k(t) = N_k(t)/\xi'_k \quad , \tag{3.52}$$

where ξ'_k is a constant which depends upon the detection efficiency, the transition probability of the branch observed, the data-accumulation period, the slit width, etc. Thus the various $I_k(t)$ are Arbitrarily-Normalized Decay Curves (ANDC) and $\xi_k = \xi'_j/\xi'_n$ is the undetermined parameter which normalizes the j^{th} cascade relative to the primary. If all ANDC are measured with a common time base and initialization, (3.51) becomes [3.146]

$$dI_n/dt = \sum_j \xi_j I_j(t) - \alpha_n I_n(t) \quad , \tag{3.53}$$

which represents a separate linear relationship connecting α_n and the various ξ_j for each instant of time, with coefficients obtainable directly from the measured ANDC. Here the empirical decay curves themselves, rather than their approximate mathematical representations, are the fitting functions, and cascade mean lives occur only implicitly and are not determined. Equation (3.53) provides as many independent linear relationships as there are data channels which can be satisfied simultaneously by a standard multiple linear regression [3.122], which analytically minimizes S^2 in

$$S^2 = \sum_i (y_i - \sum_k a_k x_{ki})^2 \quad . \tag{3.54}$$

There is a choice in the possible definitions of the variables y_i and x_{ki}, which can provide alternative approaches, depending upon the accuracy of the data. If the statistical accuracy is sufficient to permit a numerical differentiation of the primary decay-curve, the variables may be defined directly from (3.53) as

$$y_i = \sqrt{W_i}\ \dot{I}_n(t_i) \quad , x_{ki} = \sqrt{W_i}\ I_k(t_i), \quad k = n, j_1, j_2, \ldots \quad , \tag{3.55}$$

where $I_n = dI_n/dt$, t_i is the time coordinate of the i^{th} channel, and W_i is the weight factor (this definition allows the use of general-purpose multiple-regression subroutines, which often are not designed to accept data of explicitly varying weight). Sophisticated numerical differentiation formulae often smooth over many data points, which is neither necessary nor desirable when it is followed by least-squares fitting. Thus a crude but adequate three-point differentiation formula for quasi-exponential

data of equal spacing AT is given by

$$I(t) = I(t)\ \ell n[I(t+\Delta T)/I(t-\Delta T)]/(2\Delta T) \quad . \tag{3.56}$$

If we assume uncorrelated statistical errors (neglecting the error correlation between I_n and I,), a satisfactory weight-factor is given by

$$W_i = [(\Delta T^{-2} + \alpha_{no}^2)I_n(t_i) + \sum_j \xi_{jo}^2 I_j(t_i)]^{-1} \quad , \tag{3.57}$$

where a_{no} and ξ_{jo} are estimated values of α_n and ξ_j, not varied in the fit, but iterated if incorrectly estimated [3.147].

If the data cannot reliably be differentiated, an alternative formulation has been suggested and utilized by KOHL [3.148], CURTIS et al. [3.149], KOHL et al. [3.150], and SCHECTMAN et al. [3.151], in which both sides of (3.53) are integrated between arbitrary limits TI and T_F, and the variables of (3.54) become

$$y_i \equiv \sqrt{W_i}\ [I_n(T_F) - I_n(T_I)] \quad , \quad x_{ik} \equiv \sqrt{W_i}\int_{T_I}^{T_F} dt \quad I_k(t) \, . \tag{3.58}$$

This formulation has the disadvantage that it combines several data points in the integration, so that the number of degrees-of-freedom is not inferred directly by the number of data points, complicating the interpretation of goodness-of-fit criteria and the definition of weight factors. However, the problems of numerical differentiation can be severe, and this integration approach provides an effective means of pooling data without degrading the time-resolution of the decay-curve.

In either formulation, the number of independent relationships must greatly exceed the number of cascades for any analyzable case. Thus the applicability of this method to a given set of measurements is indicated by the goodness of the fit obtained. If one or more significant cascade decay-curves has been neglected, the analysis should produce a poor fit. Contrarily, if a given cascade is neglected and a satisfactory fit can be obtained, then its contribution to the repopulation is probably small. There are a number of ways to test the goodness-of-fit. One involves reciprocity of the fit under interchange of the role of the independent variables in the fit. In our formulation, we have chosen y_i as the axis along which deviations are minimized. If one of the other variables assumes this role, the minimization process is altered, but the values inferred for α_n and the ξ_i should be the same to within fit variances if the decay curves are truly correlated. The χ^2 test also gives a measure of goodness-of-fit, provided the weights chosen accurately reflect the uncertainties in the measurement. With appropriate weights, the regression also provides an estimate of the uncertainties in α_n and ξ_j.

The goodness-of-fit can be displayed on a graphical plot if the number of parameters can be reduced to two. As an example, consider a level 1 which has cascades from levels 2 and 3. Equation (3.53) becomes

$$dI_1/dt = \xi_2 I_2(t) + \xi_3 I_3(t) - \alpha_1 I_1(t) \quad . \tag{3.59}$$

If the ratio $e = \xi_3/\xi_2$ can be determined, either empirically or by a prior multiparameter regression, this equation can be rewritten for the i^{th} channel as

$$[-d(\ell n I_1)/dt] = \alpha_1 - \xi_2[(I_2+eI_3)/I_1]_i \quad . \tag{3.60}$$

Thus a plot of one bracketed quantity vs. the other will yield α_1 and ξ_2 as an intercept and a slope, respectively, about which the scatter of points is an obvious goodness-of-fit indicator. An example of this is shown in Fig.3.6 for the $4p\,^2P$ level in

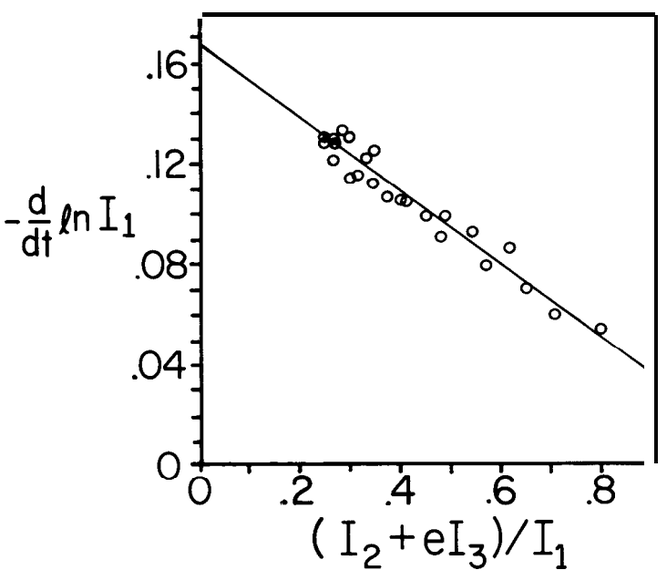

Fig.3.6 Plot of the negative logarithmic derivative of the primary level vs. the adjusted sum of its cascade decay curves for the $4p\,^2P$ level in Ca II. These quantities are linearly related, so the ordinate intercept gives a a_{4P} and the slope gives the relative normalization of the cascades to the primary

Ca II. The decay curve of $4p\,^2P$ was heavily repopulated by fast cascades from $5s\,^2S$ and $4d\,^2D$ which gave it a strong growing-in shape. This greatly hampered accurate curve fitting and could have allowed ambiguities in the assignment of mean lives if

the cascade decay-curves had not also been measured. A three-parameter regression of the three measured decay-curves was made with (3.59) which yielded values of α_1 = 0.168, ξ_2 = 0.86 and ξ_3 = 0.43. The bracketed quantities in (3.60) were then computed with e set at 0.50, and the goodness-of-fit is clear from the plot.

This method employs exact linear relationships to incorporate cascade decay-curves into the analysis of the primary decay-curve, does not involve exponential curve-fitting, and provides self-consistency checks of its validity. The method utilizes the same decay-curves as standard curve-fitting techniques, so is an additional rather than an alternative approach, which can be very useful in resolving possible ambiguities and extracting mean lives in troublesome cases.

3.7 Cascade-Free Methods

Several methods have been developed which can, in certain circumstances, completely eliminate cascade effects from fast ion-beam mean-life measurements.

3.7.1 Beam-Foil Coincidence Techniques

Although photon-photon coincidence techniques have provided a method for making cascade-free mean-life measurements in nuclear physics and in electron-beam excited-atom studies, low light-levels make its application very difficult in the beam-foil case. However, this technique has been used successfully by MASTERSON and STONER [3.152] to measure one mean life for which a single cascade dominates. In their experiment, the true coincidence rate was only about 1/40 of the chance coincidence rate, but they were able to subtract the chance coincidences by use of a single-channel approach (a multichannel analyzer recorded both the fixed-delay-window peak and surrounding background, permitting an estimation of the background under the peak). In order to obtain a signal 3 times the statistical fluctuations in the chance coincidences, about $(3x40)^2$ = 14400 total coincidences were required per channel, the accumulation of which took approximately 40 hours per point, or 10 days of running time for a 6-point decay curve. Although these times indicate the great difficulties inherent in such a measurement, the results clearly demonstrate that the measurement is possible. The method has a unique advantage in that it can establish a correlation between the cascade and primary transitions, and can therefore be used to verify level schemes.

3.7.2 Use of Alignment to Discriminate Against Cascades

It is well known that beam-foil excitation often produces alignment in substate populations, which (as shown in Subsection 3.4.3) gives rise to linear polarization of the radiation emitted into limited solid angles. For a given level, the population consists of two incoherent non-interacting portions: (a) the "remnant" of the initial

foil excitation, and (b) the "repopulation" added by cascades. Since the sublevels all decay with the same mean life, the remnant retains its initial alignment, while the repopulation contains whatever alignment it transfers from the higher-lying states (which in general is reduced by the $\Delta M = 0, \pm 1$ selection rules). NEDELEC [3.153] has obtained general expressions for the transfer of alignment by cascades, which indicate that it is in most cases small. Let us therefore consider a case in which cascade-induced alignment is negligible, either because the cascade levels are not aligned, or because their alignment is not efficiently transferred. In this case (3.17) and (3.18) for the sublevels can be written as

$$N_{\gamma JM}(t) = [N_{\gamma JM}(0) - \sum_k \beta_k] \exp(-\alpha_{\gamma J} t) + \sum_k \beta_k \exp(-\alpha_k t) \quad , \tag{3.61}$$

where k is summed over the cascades, and since the cascade contributions to all sublevels of the primary level are the same, the β_k are M-independent. This expression suggests an analysis technique which can be understood by consideration of (3.30a) and (3.30b). If the light is viewed at $\theta = 90°$ through parallel and perpendicular polarizers, the results being corrected for instrumental polarization, the difference in intensities yields

$$\Delta I'' / \eta^{\parallel} - \Delta I^{\perp} / \eta^{\perp} = \sum_M N_{\gamma JM}(t) [3A_{\gamma JM, \gamma' J' M} - A_{\gamma J \ \gamma' j'}] \quad . \tag{3.62}$$

Substituting in (3.61) and using the sum rule of (3.31), we find that the k terms vanish, leaving the expression

$$\Delta I'' / \eta^{\parallel} - \Delta I^{\perp} / \eta^{\perp} = \left\{ \sum_M N_{\gamma JM}(0) [3A_{\gamma JM, \gamma' J' M} - A_{\gamma J, \gamma' J'}] \right\} \exp(-\alpha_{\gamma J} t) \quad , \tag{3.63}$$

so the difference between the two multiexponential decay curves should be a single exponential with the mean life of the primary level. This approach has been used by BERRY et al. [3.154]. After subtracting the unpolarized background and correcting for instrumental polarizations (which were made small by use of a scrambler) the two multiexponential polarization decay-curves of the Li II 47878 transition (indicated by hollow circles) were subtracted to give a single exponential curve (shown by solid circles). Although the polarization was small, tolerable accuracies in the subtracted differences were achieved by keeping statistical uncertainties in the measured decay curves below 1%. They also used this technique to remove blending effects in hydrogenic decay curves. The S-state portions, being unpolarized, cancelled on subtraction, and higher angular momentum state polarizations showed an energy dependence. Thus for the He II 3-5 transition the 5f mean life dominated the subtracted decay curve at

300 keV, while the 5p mean life dominated at 1.5 MeV. For BERRY et al.'s results, see Fig.3.7.

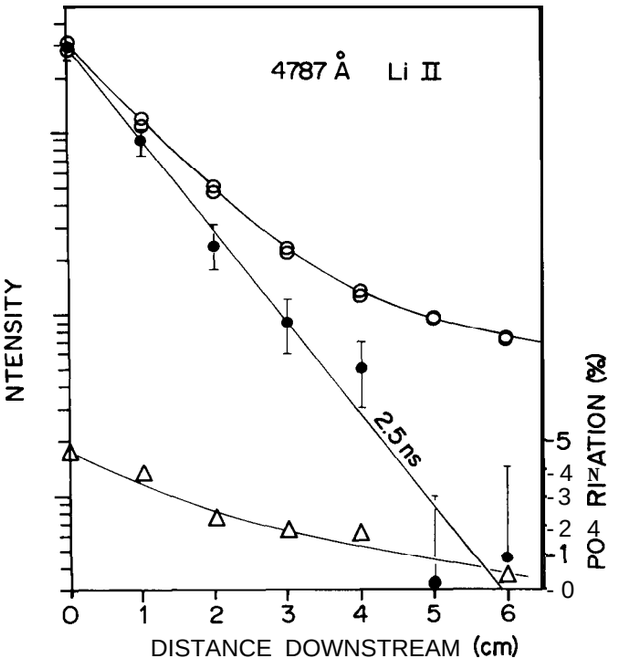

Fig.3.7 Decay curves for the Li II $3p\ ^1P - 4d\ ^1D$ transition measured in polarizations parallel (upper O) and perpendicular (lower O) to the beam axis and their subtracted difference (●), multiplied by 10 for common (arbitrary) normalization. The lower part of the figure (△) shows the change of polarization as the cascading fraction increases

An automated system for measuring (3.63) directly, coupling rotating polarization analyzers to a phase-sensitive detector, has been used by SCHECTMAN [3.155], which may make this specialized technique more generally applicable. A similar technique, utilizing the lack of cascade-induced alignment to suppress cascade effects in the beam-foil Hanle effect has been utilized by LIU and CHURCH [3.156] and CHURCH and LIU [3.157].

3.7.3 Laser Excitation

One of the most promising new techniques which has been used for mean-life measurements is selective excitation of a fast ion beam in flight by an intersecting laser beam. This technique provides cascade-free decay curves, and shares with beam-foil

excitation its high isotopic purity and low particle density, while avoiding the problems of beam energy spread due to losses in the foil. The first experiment of this type was performed by ANDRÄ et al. [3.158,159] who Doppler-tuned an argon-ion laser through 9Å by variation of the intersection angle between the beams, which then corresponded to a Ba II resonance transition. This technique can routinely yield mean lives good to better than 1%, and is being extended through the use of tunable dye lasers and beam excitation within a laser cavity. However, in this form, the technique cannot be applied to levels which are not optically excitable from the ground state, and does not have the access to highly ionized and multiply-excited states of a beam-foil source.

Some of the limitations of this method can be eliminated by a variation developed by HARDE and GUTHÖHRLEIN [3.160], in which the ion beam is pre-excited in a gas cell, (or foil) before receiving further excitation from a continuous-wave intracavity dye laser, which is chopped at 82 Hz. Although the total emitted intensity is not cascade-independent, the difference between the chopped decay curves, measured with a digital lock-in photon counting system, is, and decays as a single exponential at points downstream from the laser. To verify this, consider a component transition between an upper state n and a lower state k (the laser does not pump the various sublevels equally, so the components must be considered separately). Without laser excitation, the upper state population $N_n^0(t)$ is governed by

$$dN_n^0/dt = \sum_i N_i(t)A_{in} - N_n^0(t)\,\alpha_n \quad . \tag{3.64}$$

With laser excitation, the population becomes $N_n^1(t)$, governed by

$$dN_n^1/dt = W_{kn}[N_k^1(t) - N_n^1(t)] + \sum_i N_i(t)A_{in} + N_n^1(t)\,\alpha_n \quad , \tag{3.65}$$

where W_{kn} is the stimulated transition probability [3.161]. Notice that the cascade contributions are the same in either case, so if we subtract (3.64) from (3.65) we obtain

$$\left(\frac{d}{dt} + \alpha_n\right)\left[N_n^1(t) - N_n^0(t)\right] = W_{kn}\left[N_k^1(t) - N_n^1(t)\right] \quad . \tag{3.66}$$

Thus during the dwell time in the laser when $W_{kn} \neq 0$ there will be a pumping (either up or down) proportional to the <u>difference</u> in population between the upper and lower levels. Thus it is important to place the laser at an appropriate distance downstream from the pre-exciter to optimize that difference. Downstream from the laser, where $W_{kn} = 0$, (3.66) yields a single exponential of inverse mean life α_n, if the upper level populations with and without the laser differ. This method has so far been applied only to ground state and metastable state cases, but it may well be one of the major applications of beam-foil methods in the future.

3.8 Concluding Remarks

In the past few years the measurement and analysis of beam-foil decay curves has been substantially improved and mean lives measured by this technique must be considered to be among the most reliable values presently available. Cascade effects, once a serious problem, are now correctly accounted for in the vast majority of cases. Beam-foil measurements have provided more atomic mean-life information than all other direct measurement techniques combined, even for neutral and singly-ionized atoms for which other higher intensity sources are available. Post-foil optical pumping using tunable dye lasers offers an extremely interesting possibility, which may lead to new types of lifetime measurements. The beam-foil source has a unique ability to produce highly-ionized and multiply-excited states of virtually any atom, and lifetime measurements in such systems present a very fertile area for future research.

Acknowledgments

I am grateful to Dr. J. Bromander for permission to use his published figure and to Dr. G. Sdrensen for making available unpublished materials. Many helpful suggestions have been gained from discussions with Professors W. S. Bickel, D. G. Ellis, C. G. Montgomery, H. J. Simon, Wm. Hayden Smith, and with Dr. J. Hansen. I am indebted to Professors H. G. Berry, I. Martinson, E. H. Pinnington and R. M. Schectman for their critical reading of the first draft, and to Deborah MacDonald for her help in the preparation of the final manuscript.

References

3.1 P. L. Smith: Nucl. Instr. and Meth. 110, 395 (1973)

3.2 D. C. Morton, J. F. Drake, E. B. Jenkins, J. B. Rogerson, L. Spitzer, D. G. York: Astrophys. J. 181, L103 (1973)

3.3 D. C. Morton, J. F. Drake, E. B. Jenkins, J. B.. Rogerson, L. Spitzer, D. G. York: Astrophys. J. 181, L110 (1973)

3.4 D. Layzer, R. H. Garstang: In *Annual Reviews of Astronomy and Astrophysics,* Vol. 6, ed. by L. Goldberg (Annual Reviews, Inc., Palo Alto 1968)pp.449-494

3.5 R. J. S. Crossley: In *Advances in Atomic and Molecular Physics,* Vol. 5, ed. by D. R. Bates, I. Estermann (Academic Press, New York, London 1969)pp. 237-296

3.6 A. W. Weiss: Nucl. Instr. and Meth. 90, 121 (1970)

3.7 0. Sinanoğlu: Nucl. Instr. and Meth. 110, 193 (1973)

3.8 M. W. Smith, W. L. Wiese: Astrophys. J. Suppl. Ser. 23, 103 (1971)

3.9 T. Andersen, A. Kirkegård Nielsen, G. Sørensen: Nucl. Instr. and Meth. 110, 143 (1973)

3.10 A. C. G. Mitchell, M. W. Zemansky: *Resonance Radiation and Excited Atoms* (Cambridge University Press, London, New York 1961)pp.96-153

3.11 E. W. Foster: Rept. Progr. Phys. 27, 469 (1964)

3.12 W. R. Bennett, Jr., P. J. Kindlmann, G. N. Mercer: Appl. Opt. Suppl. 2, 34 (1965)

3.13 K. Ziock: In *Methods of Experimental Physics,* Vol. 4B, ed. by V. W. Hughes, H. L. Schultz (Academic Press, New York, London 1967)pp. 214-225

3.14 W. L. Wiese: In *Methods of Experimental Physics,* Vol. 7A, ed. by B. Bederson, W. L. Fite (Academic Press, New York, London 1968)pp. 117-141

3.15 A. Corney: In *Electronics and Electron Physics,* Vol. 29, ed. by L. Marton, (Academic Press, New York, London 1970)pp.115-231

3.16 P. Erman, Physica Scripta 11, 65 (1975)

3.17 Procedures almost identical to our modern lifetime determinations were used by A. V. Harcourt, W. Esson: Phil. Trans. Roy. Soc. London 156, 193 (1866). They made very precise measurements of monomolecular chemical reaction rates and fitted their results to one and two exponentials. In an appendix, Esson correctly solved the population differential equation for both a branched cascade and for a blend. However, the extracted rate constants were strongly dependent upon temperature and concentration and could not then be given fundamental meaning.

3.18 E. Rutherford: Phil. Mag. 49, 161 (1900)
Similar qualitative results had been obtained with chemically-separated sources a few months earlier by J. Elster, H. Geitel: Ann. Physik 69, 83 (1899)

3.19 E. Rutherford, F. Soddy: J. Chem. Soc. 81, 321, 837 (1902)

3.20 E. Rutherford, F. Soddy: Phil. Mag. 4, 370, 569 (1902)

3.21 E. Rutherford, F. Soddy: Phil. Mag. 5, 576 (1903)

3.22 E. Rutherford: Phil. Trans. Roy. Soc. London A 204, 169 (1904)

3.23 F. Soddy: Nature 69, 297 (1904)
Soddy later wrote that, "So far as I know, the period of average life was first deduced by Mr. J. K. H. Inglis, to whom I put the problem." [F. Soddy: The *Interpretation of Radiwn and the Structure of the Atom,* 4th ed. (G. P. Putnam's Sons, New York 1920)p. 113]

3.24 E. von Schweidler: *Congrès Intemat. Radiologie* (Liege 1905) Chapt.15, Section 1

3.25 M. von Laue: *History of Physics* (Academic Press, New York 1950)p. 111

3.26 H. Bateman: Proc. Cambridge Phil. Soc. 16, 423 (1910)

3.27 W. Wien: Ann d. Phys. 30, 369 (1909)

3.28 L. Dunoyer: Le Radium 10, 400 (1913)

3.29 A. Einstein: Verhandl. Deut. Phys. Ges. 18, 318 (1916)

3.30 A. Einstein: Phys. Z. 18, 121 (1917)

3.31 W. Wien: Ann. Physik 60, 597 (1919)

3.32 L. J. Curtis: J. Opt. Soc. Am. 63, 105 (1973)

3.33 P. A. M. Dirac: Proc. Roy Soc. A112, 661 (1926)

3.34 P. A. M. Dirac: Proc. Roy Soc. A114, 243 (1927)

3.35 A summary of papers, published during 1909-1927, is given by W. Wien: In *Handbuch der Experimentalphysik*, Vol. 14, ed. by W. Wien, F. Harms (Akademische Verlagsges, Leipzig 1927)

3.36 A. J. Dempster: Phys. Rev. 15, 138 (1920)

3.37 A. J. Dempster: Astrophys. J. 57, 193 (1923)

3.38 J. S. McPetrie: Phil. Mag. 1, 1082 (1926)

3.39 H. Kerschbaum: Ann. Physik 79, 465 (1926)

3.40 H. Kerschbaum: Ann. Physik 83, 287 (1927)

3.41 E. Rupp: Ann. Physik 80, 528 (1926)

3.42 R. d'E. Atkinson: Proc. Roy. Soc. 116, 81 (1927)

3.43 I. Wallerstein: Phys. Rev. 33, 800 (1929)

3.44 H. D. Koenig, A. Ellett: Phys. Rev. 39, 576 (1932)

3.45 P. Soleillet: Compt. Rend. 194, 783 (1932)

3.46 Z. Bay, G. Papp: Rev. Sci. Instr. 19, 565 (1948). (These investigations were carried out in 1943-44, but could not be published because of wartime circumstances).

3.47 S. Heron, R. W. P. McWhirter, E. H. Rhoderick: Nature 174, 564 (1954)

3.48 S. Heron, R. W. P. McWhirter, E. H. Rhoderick: Proc. Roy. Soc. (London) A234, 565 (1956)

3.49 E. Brannen, F. R. Hunt, R. H. Adlington, R. W. Nicholls: Nature 175, 810 (1955)

3.50 W. R. Bennett, Jr.: In Advances in *Quantum Electronics*, ed. by J. Singer (Columbia University Press, New York 1961)

3.51 L. Kay: Phys. Letters 5, 36 (1963)

3.52 S. Bashkin: Nucl. Instr. and Meth. 28, 88 (1964)

3.53 E. U. Condon, G. H. Shortley: *The Theory of Atomic Spectra* (Cambridge University Press, London 1957)

3.54 D. G. Ellis: J. Opt. Soc. Am. 63, 1232 (1973)

3.55 R. Ladenburg, F. Reiche: Naturwiss. 27, 584 (1923)

3.56 B. W. Shore, D. H. Menzel: *Principles of Atomic Spectra* (John Wiley and Sons, New York 1968)

3.57 L. R. Maxwell: Phys. Rev. 38, 1664 (1931)

3.58 D. C. Morton, W. H. Smith: Astrophys. J. Suppl. Ser. 26, 333 (1973)

3.59 C. Laughlin, A. Dalgarno: Phys. Rev. A 8, 39 (1973)

3.60 e.g., W. R. Bennett, P. J. Kindlmann, G. N. Mercer: Appl. Opt. Suppl. 2, 34 (1965)

3.61 J. Z. Klose: Phys. Rev. 141, 181 (1966)

3.62 W. R. Bennett, P. J. Kindlmann: Phys. Rev. 149, 38 (1966)

3.63 G. M. Lawrence: Phys. Rev. 175, 40 (1968)

3.64 L. Barrette, R. Drouin: Physica Scripta 10, 213 (1974)

3.65 J. Bromander: Nucl. Instr. and Meth. 110, 11 (1973)

3.66 I. Martinson, A. Gaupp: Physics Reports 15C, 113 (1974)

3.67 S. Bashkin, In *Progress in Optics*, Vol. XII, ed. by E. Wolf (North-Holland, Amsterdam 1974)pp. 289-344

3.68 I. Martinson: Nucl. Instr. and Meth. 110, 1 (1973)

3.69 I. Martinson: Physica Scripta 9, 281 (1974)

3.70 H. G. Berry: Physica Scripta (to be published)

3.71 Many laboratories evaporate their own foils; others obtain them from suppliers such as the Arizona Carbon Foil Company, Tucson, Arizona, or the Yissum Research Development Company, Hebrew University, Jerusalem. One might remark that foil thickness is often unspecified or poorly determined

3.72 L. Lundin has incorporated much of the precision technology of ruling engines into foil-drive design

3.73 J. O. Stoner, Jr., J. A. Leavitt: Appl. Phys. Letters 18, 368 (1971)

3.74 J. O. Stoner, Jr., J. A. Leavitt: Appl. Phys. Letters 18, 477 (1971)

3.75 J. O. Stoner, Jr., J. A. Leavitt: Optica Acta 20, 435 (1973)

3.76 J. A. Leavitt, J. W. Robson, J. O. Stoner, Jr.: Nucl. Instr. and Meth. 110, 423 (1973)

3.77 E. L. Chupp, L. W. Dotchin, D. J. Pegg: Phys. Rev. 175, 44 (1968)

3.78 W. S. Bickel, R. Buchta: Physica Scripta 9, 148 (1974)

3.79 L. J. Curtis, H. G. Berry, J. Bromander: Physica Scripta 2, 216 (1970)

3.80 L. Kay: Physica Scripta 5, 139 (1972)

3.81 R. C. Etherton, L. M. Beyer, W. E. Maddox, L. B. Bridwell: Phys. Rev. A 2, 2177 (1970)

3.82 D. Halliday: Introductory *Nuclear* Physics, 2nd ed. (Wiley, New York, London 1960)p. 247

3.83 E. H. Pinnington: Nucl. Instr. and Meth. 90, 93 (1970)

3.84 R. M. Schectman, L. J. Curtis, C. Strecker, K. Kormanyos: Nucl. Instr. and Meth. 90, 197 (1970)

3.85 J. B. Marion: Rev. Mod. Phys. 38, 660 (1966)

3.86 J. O. Stoner, Jr.: J. Appl. Phys. 40, 707 (1969)

3.87 J. Lindhard, M. Scharff, H. E. Schiøtt: Kgl. Danske Videnskab. Selskab, Mat.-Fys. Medd. 33, 14 (1963)

3.88 L. C. Northcliffe, R. F. Schilling: Nucl. Data Tables A7, 233 (1970)

3.89 K. B. Winterbon: AECL 3194 (Scientific Document Distribution Office, Chalk River, Canada 1968)

3.90 P. Hvelplund, E. Laegsgård, J. O. Olsen, E. H. Pederson: Nucl. Instr. and Meth. 90, 315 (1970)

3.91 c. L. Cocke, B. Curnutte, J. H. Brand: Astron. and Astrophys. 15, 299 (1971)

3.92 W. R. Bennett, Jr., P. J. Kindlmann: Phys. Rev. 149, 38 (1966)

3.93 K. E. Donnelly, P. J. Kindlmann, W. R. Bennett, Jr.: IEEE J. Quant. Electr. QE10, 848 (1974)

3.94 R. D. Kaul : J. Opt. Soc. Am. 56, 1262 (1966)

3.95 G. H. Nussbaum, F. M. Pipkin: Phys. Rev. Letters 19, 1089 (1967)

3.96 R. E. Imhof, F. H. Read: Chem. Phys. Letters 3, 652 (1969)

3.97 L. J. Curtis, W. H. Smith: Phys. Rev. A 9, 1537 (1974)

3.98 M. Dufay: Nucl. Instr. and Meth. 110, 79 (1973)

3.99 E. H. Pinnington, A. E. Livingston, J. A. Kernahan: Phys. Rev. A 9, 1004 (1974)

3.100 A. Dalgarno: Nucl. Instr. and Meth. 110, 183 (1973)

3.101 C. Laughlin, M. N. Lewis, Z. J. Horak: J. Opt Soc. Am. 63, 736 (1973)

3.102 F. Weinhold: J. Chem. Phys. 54, 1874 (1971)

3.103 M. T. Anderson, F. Weinhold: Phys. Rev. A 10, 1457 (1974)

3.104 L. J. Curtis: J. Opt. Soc. Am. 64, 495 (1974)

3.105 L. J. Curtis: Amer. J. Phys. 36, 1123 (1968)

3.106 N. H. Gale: Nucl. Phys. 38, 252 (1962)

3.107 G. M. Lawrence: Phys. Rev. A 2, 397 (1970)

3.108 W. P. Helman: Int. J. Radiat. Phys. Chem. 3, 283 (1971)

3.109 V. A. Ankudinov, S. V. Bobashev, E. P. Andreev: Zh. Eksper. I. Teor. Fiz. 48, 40 (1965)

3.110 V. A. Ankudinov, S. B. Bobashev, E. P. Andreev: Sov. Phys. JETP 21, 26 (1965)

3.111 W. S. Bickel, A. S. Goodman: Phys. Rev. 148, 1 (1966)

3.112 L. J. Curtis, R. M. Schectman, J. L. Kohl, D. A. Chojnacki, D. R. Shoffstall: Nucl. Instr. and Meth. 90, 207 (1970)

3.113 B. L. Moiseiwitsch, S. J. Smith: Rev. Mod. Phys. 40, 238 (1968), with erratum 41, 574 (1969)

3.114 W. Hanle: Z. Instrumentenk. 51, 488 (1931)

3.115 J. Orear: *Notes on Statistics for Physicists,* Report UCRL-8417 (University of California Radiation Lab., Berkeley 1958)

3.116 F. Grard: Nucl. Instr. and Meth. 34, 242 (1965)

3.117 P. H. R. Orth, W. R. Falk, G. Jones: Nucl. Instr. and Meth. 65, 301 (1968)

3.118 A. H. Jaffey: Nucl. Instr. and Meth. 81, 155 (1970)

3.119 A. H. Jaffey: Nucl. Instr. and Meth. 81, 253 (1970)

3.120 A. H. Jaffey: Nucl. Instr. and Meth. 81, 218 (1970)

3.121 G. F. Lee, G. Jones: Nucl. Instr. and Meth. 91, 665 (1971)

3.122 P. R. Bevington: *Data Reduction and Error Analysis for the Physical Sciences* (McGraw-Hill, New York 1969)

3.123 D. W. Marquardt: J. Soc. Ind. Appl. Math. 11, 431 (1963)

3.124 C. Daniel, F. S. Wood, J. W. Gorman: *Fitting Equations to Data - Computer Analysis of Multifactor Data for Scientists and Engineers* (Wiley, New York London 1971)
Program GAUSHAUS 360 D-13.6.007 available from Share Program Library Agency, Research Triangle Park, North Carolina 27709

3.125 R. Fletcher: *A Modified Marquardt Subroutine for Non-Linear Least Squares,* AERE report, R.6799 (Harwell Atomic Energy Res. Estab.)
Program VB01A available Harwell Subroutine Library, Harwell, England

3.126 R. H. Moore, R. K. Ziegler: *The Solution of the General Least-Squares Problem with Special Reference to High Speed Computers,* Report LA-2367 (Los Alamos Scientific Laboratory, Los Alamos, New Mexico)

3.127 D. J. G. Irwin, A. E. Livingston: Computer Phys. Comm. 7, 95 (1974), Program HOMER

3.128 P. C. Rogers: MIT Lab. Nucl. Sci. Tech. Report No. 76, NYO 2303, Program FRANTIC

3.129 C. Lanczos: *Applied Analysis* (Prentice-Hall, Englewood Cliffs, New Jersey 1956)pp. 272-282

3.130 Problems with reliable numerical differentiation of statistically fluctuating data can be severe, but satisfactory results have been obtained using numerical filtering programs, e.g., A. Savitsky, M. J. E. Golay: Analytical Chem. 36, 1627 (1964)

3.131 L. J. Curtis, I. Martinson, R. Buchta: Physica Scripta 3, 197 (1971)

3.132 A. Denis, P. Ceyzériat, M. Dufay: J. Opt. Soc. Am. 60, 1186 (1970)

3.133 D. G. Gardner, J. C. Gardner, G. Laush, W. W. Meinke: J. Chem. Phys. 31, 978 (1959)

3.134 J. W. Cooley, J. W. Tukey: Math. Comp. 19, 297 (1965)

3.135 J. Schlesinger: Nucl. Instr. and Meth. 106, 503 (1973)

3.136 Z. Bay: Phys. Rev. 77, 419 (1950)

3.137 z. Bay, V. P. Henri, H. Kanner: Phys. Rev. 100, 1197 (1955)

3.138 R. D. Dyson, I. Isenberg: Biochem. 10, 3233 (1971)

3.139 I. Isenberg, R. D. Dyson: Biophys. J. 9, 1337 (1969)

3.140 R. Schuyler, I. Isenberg: Rev. Sci. Instr. 42, 813 (1971)

3.141 J. Yguerabide: In *Methods in Enzymology,* Vol. XXVI, ed. by C. H. W. Hirs, S. N. Timasheff (Academic Press, New York, London 1972)pp. 498-578

3.142 L. J. Curtis: In *Proceedings of the Second European Conference on Beam-Foil Spectroscopy and Connected Topics,* ed. by M. Dufay (University of Lyon, Lyon, France (1971)

3.143 L. Kay: Physica Scripta 5, 138 (1972)

3.144 I. Martinson, A. Gaupp, L. J. Curtis: J. Phys. B 7, L463 (1974)

3.145 R. Tielert, H. H. Bukow: Z. Physik 264, 119 (1973)

3.146 L. J. Curtis, H. G. Berry, J. Bromander,: Phys. Letters 34A, 169 (1971)

3.147 D. R. Barker, L. M. Diana: Am. J. Phys. 42, 224 (1974)

3.148 J. L. Kohl: Phys. Letters 24A, 125 (1967)

3.149 L. J. Curtis, R. M. Schectman, J. L. Kohl, D. R. Shoffstall: Nucl. Instr. and Meth. 90, 207 (1970)

3.150 J. L. Kohl, L. J. Curtis, R. M. Schectman, D. A. Chojnacki: J. Opt. Soc. Am. 61, 1656 (1971)

3.151 R. M. Schectman, L. J. Curtis, D. A. Chojnacki: J. Opt. Soc. Am. 63, 99 (1973)

3.152 K. D. Masterson, J. 0. Stoner, Jr.: Nucl. Instr. and Meth. 110, 441 (1973)

3.153 0. Nedelec: J. Physique 27, 660 (1966)

3.154 H. G. Berry, L. J. Curtis, J. L. Subtil: J. Opt. Soc. Am. 62, 771 (1972)

3.155 R. M. Schectman: private communication

3.156 C. H. Liu, D. A. Church: Phys. Rev. Letters 29, 1208 (1972)

3.157 D. A. Church, C. H. Liu: Nucl. Instr. and Meth. 110, 147 (1973)

3.158 H. J. Andrä, A. Gaupp, W. Wittmann: Phys. Rev. Letters 31, 501 (1973)

3.159 H. J. Andrä, A. Gaupp, K. Tillmann, W. Wittmann: Nucl. Instr. and Meth. 110, 453 (1973)

3.160 H. Harde, G. Guthöhrlein: Phys. Rev. A 10, 1488 (1974)

3.161 A. E. Siegman: An *Introduction to Lasers and Masers* (McGraw-Hill, New York 1971)p. 256